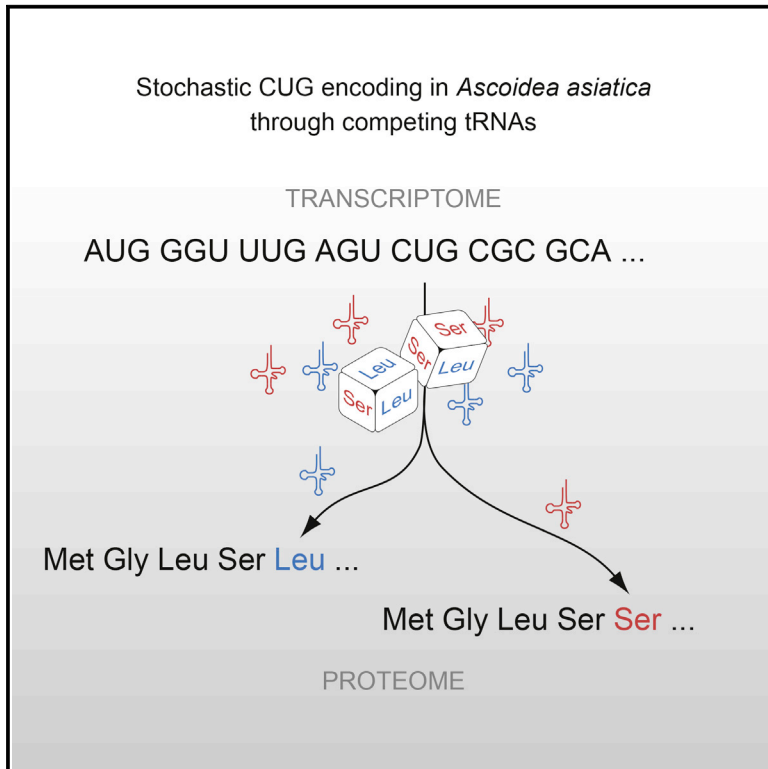


Current Biology

Endogenous Stochastic Decoding of the CUG Codon by Competing Ser- and Leu-tRNAs in *Ascoidea asiatica*

Graphical Abstract



Authors

Stefanie Mühlhausen,
Hans Dieter Schmitt, Kuan-Ting Pan,
Uwe Plessmann, Henning Urlaub,
Laurence D. Hurst, Martin Kollmar

Correspondence

mako@nmr.mpibpc.mpg.de

In Brief

Mühlhausen et al. discover that *Ascoidea asiatica* stochastically encodes CUG as both serine and leucine, which is most likely caused by two competing tRNAs. This is the first example where the non-ambiguity rule of the genetic code is broken. To minimize its effect, *A. asiatica* uses CUG only rarely and never at conserved sequence positions.

Highlights

- *Ascoidea asiatica* stochastically encodes CUG as leucine and serine
- It is the only known example of a proteome with non-deterministic features
- Stochastic encoding is caused by competing tRNA^{Leu}(CAG) and tRNA^{Ser}(CAG)
- *A. asiatica* copes with stochastic encoding by avoiding CUG at key positions

Endogenous Stochastic Decoding of the CUG Codon by Competing Ser- and Leu-tRNAs in *Ascoidea asiatica*

Stefanie Mühlhausen,¹ Hans Dieter Schmitt,² Kuan-Ting Pan,³ Uwe Plessmann,³ Henning Urlaub,^{3,4} Laurence D. Hurst,¹ and Martin Kollmar^{5,6,*}

¹The Milner Centre for Evolution, Department of Biology and Biochemistry, University of Bath, Claverton Down, Bath, BA2 7AY, UK

²Department of Neurobiology, Max Planck Institute for Biophysical Chemistry, Am Fassberg 11, 37077 Göttingen, Germany

³Bioanalytical Mass Spectrometry, Max Planck Institute for Biophysical Chemistry, Am Fassberg 11, 37077 Göttingen, Germany

⁴Bioanalytics Group, Department of Clinical Chemistry, University Medical Center Göttingen, Robert Koch Strasse 40, 37075 Göttingen, Germany

⁵Group Systems Biology of Motor Proteins, Department of NMR-Based Structural Biology, Max Planck Institute for Biophysical Chemistry, Am Fassberg 11, 37077 Göttingen, Germany

⁶Lead Contact

*Correspondence: mako@nmr.mpibpc.mpg.de

<https://doi.org/10.1016/j.cub.2018.04.085>

SUMMARY

Although the “universal” genetic code is now known not to be universal, and stop codons can have multiple meanings, one regularity remains, namely that for a given sense codon there is a unique translation. Examining CUG usage in yeasts that have transferred CUG away from leucine, we here report the first example of dual coding: *Ascoidea asiatica* stochastically encodes CUG as both serine and leucine in approximately equal proportions. This is deleterious, as evidenced by CUG codons being rare, never at conserved serine or leucine residues, and predominantly in lowly expressed genes. Related yeasts solve the problem by loss of function of one of the two tRNAs. This dual coding is consistent with the tRNA-loss-driven codon reassignment hypothesis, and provides a unique example of a proteome that cannot be deterministically predicted.

INTRODUCTION

Genetic information, as stored in genomic DNA, is translated into proteins by ribosomes. This process needs tight control and accuracy so that the same functional protein is obtained from the same gene [1–3]. To preserve accuracy, ribosomes select for cognate aminoacyl-tRNAs matching nucleotide triplets (codons) of the mRNA and discriminate against non- and near-cognate aminoacyl-tRNAs. The correct tRNA charging is secured by highly specific aminoacyl-tRNA synthetases (aaRSs). Assuming there to be selection for “one mRNA-one protein,” it is not surprising that the genetic code is near universal, with there being only a few minor alterations. One such modification is the alternative decoding of the UGA stop codon by selenocysteine, although this affects only a few proteins [4, 5]. Genome-wide changes to the meaning of codons happened in the comparatively tiny organellar genomes of many species, but

are extremely rare in nuclear genomes [6, 7]. Except for yeasts, only stop codons are affected by nuclear codon reassignments. In addition to complete reassignments, several ciliates and a trypanosomatid have been discovered in which one or all stop codons have dual or, in case of the UGA stop codon, even three-fold meanings [8–11]. The decoding by standard amino acid, selenocysteine, or stop codon is always context specific and never ambiguous.

Yeasts from the clade comprising the Debaryomycetaceae and Metschnikowiaceae (abbreviated as “DM clade” from here on) and *Pachysolen tannophilus* are currently the only known species where a sense codon has been reassigned in nuclear genomes. They translate CUG as serine and alanine, respectively [12–15], rather than as the “universal” leucine. Recently, four genomes from another major yeast clade comprising the *Ascoidea* and *Saccharomycopsis* species (named “*Ascoidea* clade” from here on), have been sequenced [15, 16]. These were proposed to form a monophyletic clade according to a multigene analysis [17] and include *Saccharomycopsis fibuligera*, the major amylolytic yeast for food fermentation using rice and cassava [18]. In contrast to the suggested CUG decoding by leucine in *Ascoidea rubescens* [15], the Bagheera webserver for predicting yeast CUG codon translation [19] does not reveal any tRNA_{CAG} identity (CAG being the anticodon to CUG). This and lack of CUG codons at conserved sequence positions suggest a novel genetic code. To understand this better, we sought to investigate the evolutionary history of this recoding.

RESULTS

Translation of CUG Is Stochastic in *Ascoidea asiatica*

To determine the CUG codon translation in *Ascoidea* clade yeasts, we performed unbiased liquid chromatography-tandem mass spectrometry (LC-MS/MS) analyses generating approximately 5.34 million high-quality mass spectra of the following seven yeast proteomes: the four *Ascoidea* clade yeasts *A. asiatica*, *A. rubescens*, *S. fibuligera*, and *Saccharomycopsis*

Table 1. Mass Spectrometry Data Analysis

Yeast Species	Aoas (1)	Acr	Safi (1)	Sama	Bai	Cll	Nape
Mass spectra	733,673	637,651	329,041	570,823	597,939	290,859	588,199
PSMs	246,644	411,915	332,698	298,770	223,556	125,927	263,450
Non-redundant peptides	31,189	41,064	43,503	49,168	33,974	34,172	41,028
Identified proteins	2,763	3,507	3,202	3,831	3,439	3,571	3,752
Identified proteins (%)	35.94	52.60	51.74	61.00	54.39	60.16	66.67
Identified proteins with CUG	778	1,451	1,928	2,331	2,122	2,843	3,533
Identified proteins with CUG (%)	33.52	46.05	49.03	56.56	47.47	56.95	66.62
Covered CUG positions	135	449	730	1,292	1,211	2,360	8,756
PSMs covering CUGs	1,185	2,973	3,462	5,500	4,937	5,803	51,737
Non-redundant peptides covering CUGs	210	494	836	1,438	1,325	2,560	10,797
Supported CUG positions	110	361	541	1,033	930	1,835	7,801
Supported CUG positions (%)	81.48	80.40	74.11	79.95	76.80	77.75	89.09
Unambiguously translated, supported CUG positions (%) ^a	99.09	98.89	97.78	98.74	99.03	99.24	96.45
PSMs with supported CUG = Ser	418	2,038	2,192	2,984	2,635	3,031	72
PSMs with supported CUG = Leu	501	31	36	26	22	14	47
PSMs with CUG = Ser at positions also covered by PSMs with CUG = Leu	357	40	180	102	0	1	2
PSMs with CUG = Leu at positions also covered by PSMs with CUG = Ser	394	18	26	13	0	1	1
PSMs with supported CUG = Ala	0	3	1	2	5	6	31,945
PSMs with CUG = Ala at positions also covered by PSMs with CUG = Ser/Leu	0	0	0	1	0	1	361

Aoas (1), *A. asiatica* sample 1; Acr, *A. rubescens*; Safi (1), *S. fibuligera* sample 1; Sama, *S. malanga*; Bai, *B. inositovora*; Cll, *C. lusitaniae*; Nape, *N. peltata*. See also [Data S1](#) and [S2](#).

^a“Unambiguously translated” refers to all CUG positions for which only peptides with one translation were found. These not only include CUG positions translated by the expected, cognate tRNA-decoded amino acid but also CUG positions translated by other amino acids that might result from genome sequencing ambiguities and differences between sequenced and analyzed strains. For *A. asiatica*, we regard translation by both serine and leucine cognate tRNA_{CAG} as “unambiguous.”

malanga; *Babjeviella inositovora* and *Clavispora lusitaniae* from the DM clade and *Nakazawaea peltata*, which is the closest relative to *P. tannophilus* with a sequenced genome ([Table 1](#); [Figure S1](#); [Data S1](#)). To obtain peptide spectrum matches (PSMs) free of CUG-translation bias, 20 replicates for each genome annotation were generated with the CUG codon translated into a different amino acid in each replicate. Spectra searching against these databases resulted in 2.96 million PSMs (394,755 non-redundant peptide matches) with a median mass measurement error of about 408 parts per billion. We identified 31%–67% of the predicted proteins with median protein sequence coverage of 19%–27% and CUG codon recovery of 8%–23% ([Table 1](#); [Data S1](#)). To control the quality of the CUG-containing peptide identifications, we considered only those with b- and/or y-type fragment ions around CUG codon positions as fully supported. Unless otherwise stated, all numbers given below refer to fully supported CUG positions.

The *A. asiatica* coding sequences contain remarkably few CUG codons (4,936 codons as opposed to, for example, 27,696 in the DM clade yeast *C. lusitaniae* and 53,966 in *N. peltata*; [Data S1](#)). For 110 of the *A. asiatica* CUGs, we were able to resolve their translation with confidence ([Table 1](#) and [Data S1](#), sample 1). Remarkably, from the 929 PSMs covering those 110 CUG codon positions, 919 PSMs divide

into almost equal parts to leucine (501 PSMs, 53.9%; 82 CUG positions) and serine (418 PSMs, 45.0%; 65 CUG positions; [Figures 1A](#), [S1B](#), and [S1C](#); [Table 1](#); [Data S1](#)). In contrast, we find that *S. fibuligera* and *S. malanga* both primarily translate CUG as serine, as evident in the 2,192 (93.0%; *S. fibuligera* sample 1) and 2,984 (96.8%; *S. malanga*) PSMs covering 513 and 997 CUG positions translated as serine, respectively ([Figure 1A](#); [Table 1](#); [Data S1](#)). *A. rubescens* contains similarly low numbers of CUG codons as *A. asiatica* (7,359 codons), but translates them unambiguously as serine ([Figure 1A](#)). Of the 2,119 PSMs covering 361 CUG codon positions, 2,038 (96.2%; 333 CUG positions) contain CUG codons translated as serine ([Table 1](#); [Data S1](#)). Observed percentages of “only” about 95% PSMs covering correctly translated CUG codons compare to those observed in the DM clade yeasts *B. inositovora* and *C. lusitaniae* that both unambiguously translate CUG as serine: 95.3% (2,635 PSMs; 881 CUG positions) and 95.9% (3,031 PSMs; 771 CUG positions; [Table 1](#); [Data S1](#)) of PSMs are translated as serine in *B. inositovora* and *C. lusitaniae*, respectively. Rather, the majority of the PSMs with other translations represent differences between sequenced and analyzed yeast strains or base-calling and coverage-dependent genomic ambiguities, because in general about 99% of the CUG positions are unambiguous ([Table 1](#);

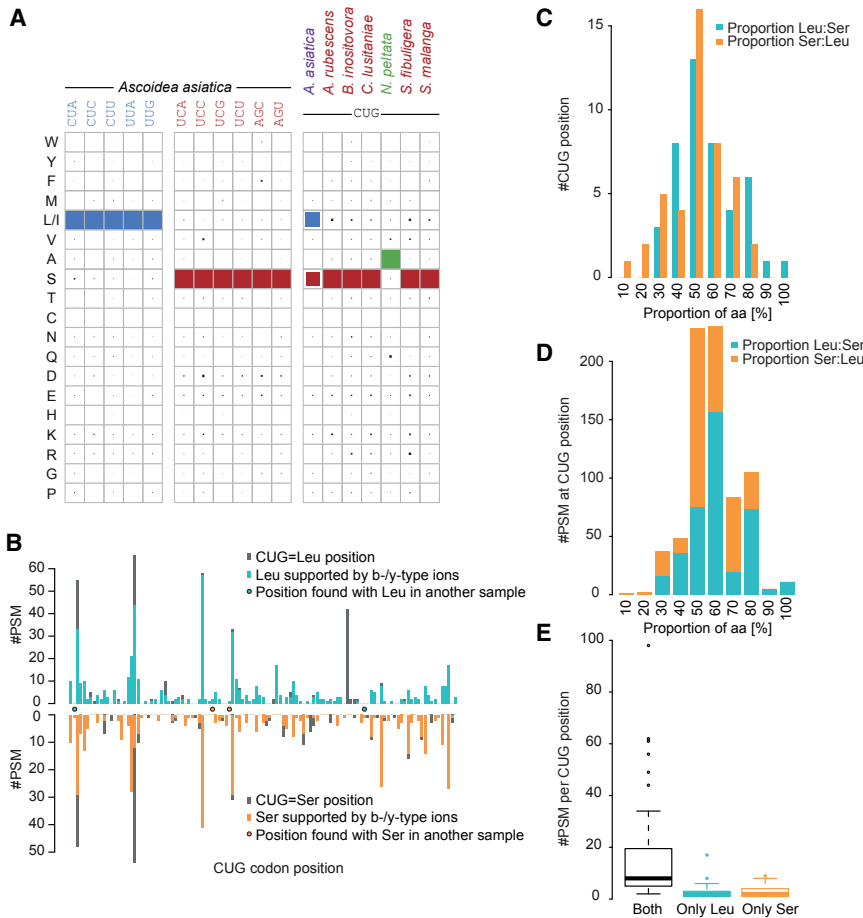


Figure 1. Stochastic Translation of the *A. asiatica* CUG Codon

(A) Translations found in PSMs at b- and/or y-type fragment ion-supported CUG codon positions. *A. asiatica* is found to translate CUG stochastically into both leucine and serine, whereas *A. rubescens*, *S. fibuligera*, and *S. malanga* translate CUG codons into serine with a level comparable to that found for *B. inositovora* and *C. lusitaniae*, which both branch inside the DM clade. *N. peltata* is the second species found to use the Pachysolen genetic code. The size of the squares corresponds to the percentage of PSMs with supported CUG with the respective translation (see also Table 1, Figure S1, and Data S1 and S2).

(B) Number of PSMs covering CUG codon positions translated as leucine or serine in *A. asiatica*: for each CUG position; the number of PSMs with a leucine (blue bars; upper) and serine (orange bars; lower) at the CUG codon is given. Gray bars denote the number of all PSMs, including those where the respective leucine or serine is not supported by b-/y-type ions. Those CUG positions that are exclusively translated into leucine or serine in this sample but also found with the respective other translation (considering positions with b-/y-type ion support only) in another sample are highlighted by dots (see also Figure S2).

(C) The proportion of CUG codons translated as serine and leucine was determined for every CUG codon position for which PSMs with both translations were available, and the number of CUGs is plotted in bins of 10%: e.g., the first bin contains all CUGs with proportions from 0% to 10%.

(D) For every CUG codon position, we separately determined the proportion of PSMs with leucine

and the proportion of PSMs with serine, and piled the number of PSMs for the respective proportion in bins of 10%. By far, most PSMs are found at positions with balanced translation, whereas only few PSMs are found at the CUG positions with unbalanced leucine-serine translation. (E) The boxplot contrasts the number of PSMs found at CUG positions with stochastic translation with the number of PSMs found at CUG positions with only leucine or serine translation.

Data S1). This ratio is neither restricted to translation as serine nor to low codon recovery, as evident in 96.5% (31,945 PSMs; 7,662 CUG positions; Table 1; Data S1) of PSMs translated as alanine in *N. peltata* (CUG codon recovery of 23.5%). Percentages of CUG codon positions supported by b-/y-type fragment ions are similar in all samples.

The unparalleled equal distribution of leucine and serine in *A. asiatica* could be caused by an endogenous, stochastic CUG codon translation or, as with stops recoded for selenocysteine, by flanking motifs determining that certain CUGs are always leucine and certain others are always serine. To test between these two possibilities, we considered what happens at any given position. At 44 CUG codon positions (40%), we found PSMs with both translations, and these positions are covered in total with almost as many PSMs with leucine (394 PSMs) as PSMs with serine (357; Figures 1B and S1C; Table 1; binomial test, $p = 0.19$). Most importantly, the distribution of PSMs with leucine and with serine is very similar for every single position (Figures 1C and 1D). At another 59 sites with fully supported CUG positions, we only recovered PSMs with either leucine (107 PSMs at 38 positions; mean of 2.8 per site) or serine

(61 PSMs at 21 positions; mean of 2.9 per site) (Figure 1E). Because we observe unique translation into either leucine or serine only at CUG positions with low coverage, it seems plausible that deeper proteomic coverage would lead to observation of stochastic translation at these sites, too.

To exclude bias from sample preparation, we generated proteomics datasets from further, independent samples grown in different media (Data S1). Analysis of these data showed similar stochastic CUG translation in all samples (Figure S2A), considerable overlap of the covered CUG positions (Figure S2B), and, most notably, recovery of some of the CUG positions translated into only serine or leucine in sample 1 with the respective other amino acid (Figure 1B). We conclude that exceptionally, *A. asiatica* has stochastic translation of CUG to two possible fates. Analysis of the other 11 leucine and serine codons, of which CUC, AGC, and UCG have similarly low codon frequency as CUG, showed these to be translated unambiguously (Figure 1A; Data S2). This indicates that cognate tRNAs are functional and unambiguous, and that the stochastic CUG translation is indeed not an artifact caused by the low CUG codon coverage in the proteomics data.

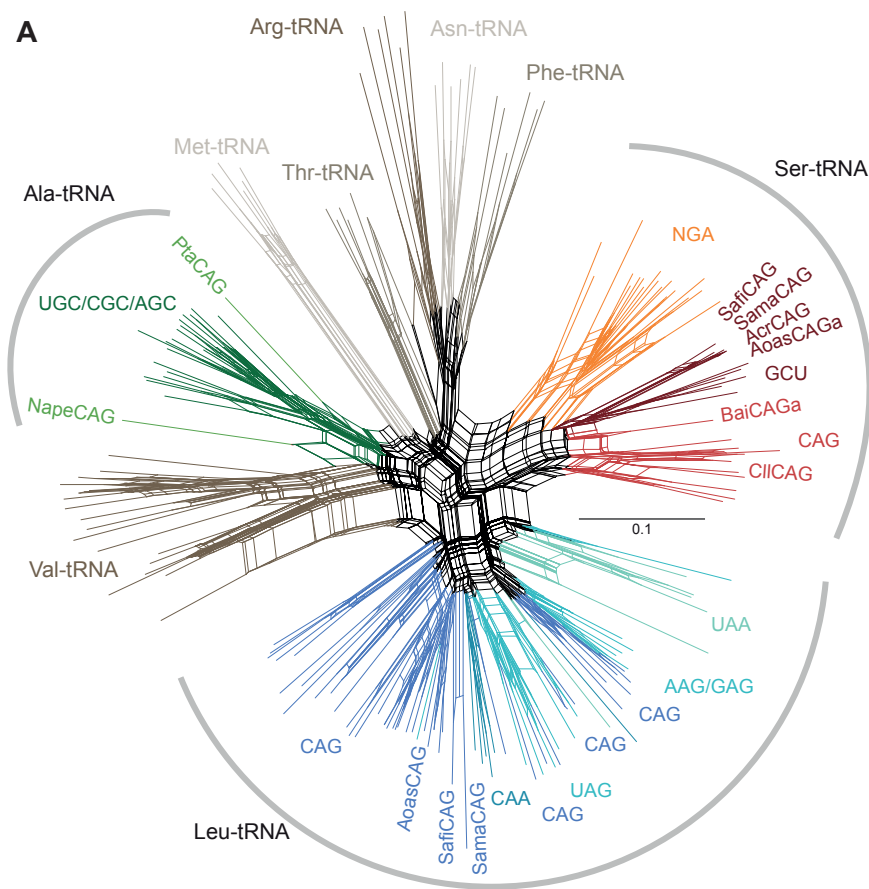
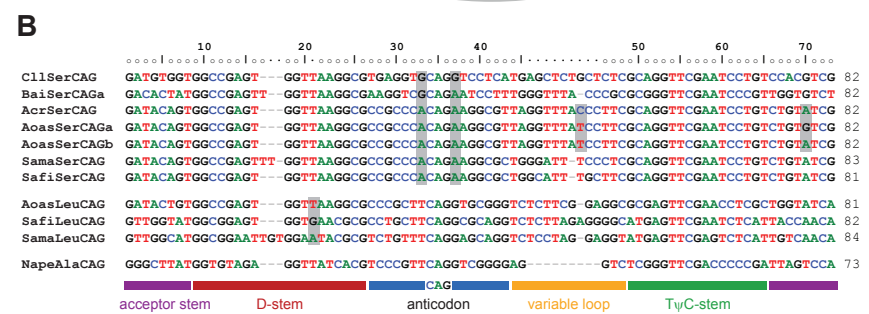


Figure 2. Yeast tRNA_{CAG} Phylogeny and Sequences

(A) An unrooted phylogenetic network of Leu-, Ser-, and Ala-tRNAs was generated with SplitsTree. Selections of Val-, Met-, Thr-, Arg-, Asn-, and Phe-tRNAs were added as outgroups. Leu-, Ser-, and Ala-tRNAs are colored by iso-acceptor. CUG-encoding tRNAs of *P. tannophilus* (Pta), *N. peltata* (Nape), *A. rubescens* (Acr), *A. asiatica* (Aoas), *S. fibuligera* (Safi), *S. malanga* (Sama), *B. inosivora* (Bai), and *C. lusitaniae* (ClI) are highlighted for better orientation. Identical tRNA identity assignments are obtained in phylogenetic analyses using maximum-likelihood and Bayesian approaches.

(B) Sequences of the tRNA_{CAG} of the analyzed species. Some nucleotides are highlighted for faster orientation. The *Saccharomycopsis* tRNA_{CAG}^{Leu} differ most strikingly from the *A. asiatica* tRNA_{CAG}^{Leu} at the important position 20a, at which the presence of purine nucleotides has been shown to dramatically reduce leucylation efficiency. Guanine nucleotides 5' and 3' of the anticodon have been shown to cause low-level misleucylation *in vitro*, but the whole-cell proteomics data of *C. lusitaniae* show unambiguous CUG translation as serine *in vivo*. The two *A. asiatica* tRNA_{CAG}^{Ser} differ from the *A. rubescens* tRNA_{CAG}^{Ser} by only 1 and 2 nt and both substitutions are at variable positions.



Stochastic Encoding of CUG Is Best Explained by Competing tRNAs

The observed stochastic CUG translation in *A. asiatica* could either result from competing tRNA_{CAG}^{Leu} and tRNA_{CAG}^{Ser} or from mis-aminoacylation of one species of tRNA_{CAG}. The fact that the translation to leucine occurs at approximately the same rate as to serine is more compatible with the competing tRNA model, as prior examples of misaminoacylation give only very weak skews. In particular, misaminoacylation has been reported for *Candida zeylanoides* and *Candida albicans*, where their tRNA_{CAG}^{Ser} might be leucylated by the LeuRS to about only 3% [20, 21]. We are aware of no example where misaminoacylation occurs at 50:50 rates. By contrast, the high rates are potentially easily explained by the presence of two competing species of functional active tRNAs. Moreover, there is precedent for two different types of tRNA for the same codon in eukaryotes, albeit

only in the context of deterministic translation, i.e., the UGA stop codon, where selenocysteine translation is extremely rare and highly specified by the selenocysteine insertion sequence (SECIS) element [8, 9]. Similarly, a few bacteria were also suggested to use sense codons for decoding selenocysteine, but in every case selenocysteine incorporation is specified by the SECIS element [22].

In silico and natural knockout analysis strongly support the viability of the competing tRNA model. The competing

tRNA model predicts the presence of at least two distinct species of tRNA_{CAG} in *A. asiatica*, and this is indeed consistent with *in silico* evidence. To resolve the identities of the *Ascoidea* yeast tRNA_{CAG}, we predicted tRNAs in 137 sequenced yeast species and performed phylogenetic analyses of tRNA_{CAG} together with representatives from all isoacceptor Leu-, Ser-, and Ala-tRNAs (Figure 2A). Notably, *A. asiatica*, *S. fibuligera*, and *S. malanga* are predicted to each contain both a tRNA_{CAG}^{Leu} and a tRNA_{CAG}^{Ser} (*A. asiatica* contains two copies of tRNA_{CAG}^{Ser}; Figure 2B). *A. rubescens*, by contrast, has only a tRNA_{CAG}^{Ser} gene. All four species encode tRNA_{UAG}^{Leu}, a tRNA that is capable of decoding CUG through wobble base pairing and has, incidentally, been lost in DM clade species.

Three species thus appear to have two species of tRNA_{CAG}, tempting the question: what is happening in the other two species, *S. fibuligera* and *S. malanga*? Here we see no evidence

for 50:50 encoding. In these two, only 1.48% and 0.39% CUG positions (of 541 and 1,033 CUG positions covered in total) show dual translation, respectively. In addition, for those eight (*S. fibuligera*) and four (*S. malanga*) CUG positions with serine-leucine ambiguity, there are 6.9 and 7.8 times more PSMs with serine than PSMs with leucine, respectively, indicating extremely low usage or efficiency of tRNA^{Leu}_{CAG} (Table 1). Thus *A. asiatica* is exceptional. Importantly, this exceptionalism is reflected in the structure of its tRNA^{Leu}_{CAG}. In contrast to their tRNA^{Ser}_{CAG}, the tRNA^{Leu}_{CAG} from *A. asiatica* and the two *Saccharomycopsis* are distinct: they group differently in the phylogenetic trees and most likely have different origins (Figure 2). Consistent with the competing tRNA model, the *Ascoidea* clade tRNA^{Leu}_{CAG} contains all elements shown to be important for leucylation specificity and accuracy, such as a methylated G37, extended variable loop, and discriminator base A73 [23–26]. The *Saccharomycopsis* tRNA^{Leu}_{CAG}, by contrast, differs from the *A. asiatica* tRNA^{Leu}_{CAG} and the Leu-tRNA consensus pattern by pyrimidine nucleotides at position 20a (Figure 2B). We also identified a tRNA^{Ala}_{CAG} in *N. peltata* that only shares the Ala-tRNA consensus nucleotides with the *P. tannophilus* tRNA^{Ala}_{CAG}, including the invariable G3-U70 base pair and the A73 discriminator base identity elements (Figure 2) [27–29]. Similar to the *Ascoidea* clade tRNA^{Leu}_{CAG}, these two tRNA^{Ala}_{CAG} have most likely been derived from different ancestors. Thus, the proteomics data evidence that the *Saccharomycopsis* yeasts and *A. rubescens* have switched CUG translation from the universal leucine to serine but that *A. asiatica* has been left with two functional tRNAs in the process.

Might it be possible that *A. asiatica* tRNA^{Ser}_{CAG} functions as an ambiguous tRNA? The presence of a unique tRNA^{Ser}_{CAG} in the close relative *A. rubescens* suggests not. This species translates CUG as serine, in accord with its unique tRNA. Importantly, the two *A. asiatica* tRNA^{Ser}_{CAG} are identical to the *A. rubescens* tRNA^{Ser}_{CAG} except for only 1 and 2 nt, respectively, and differ only in the variable loop from the *Saccharomycopsis* tRNA^{Ser}_{CAG} (Figure 2B). Importantly, all *Ascoidea* clade tRNA^{Ser}_{CAG} contain the conserved Ser-tRNA identity elements, the presence of a variable loop, and the discriminator base G73 [30, 31]. A37 has also been shown to be an antidiscriminant against the LeuRS [20]. Thus, the presence of a near-identical and unambiguously translated tRNA^{Ser}_{CAG} in *A. rubescens* provides a near-perfect natural knockout study looking at the effect of not having the tRNA^{Leu}_{CAG}. Because the two *A. asiatica* tRNA^{Ser}_{CAG} sequences are near identical to the *A. rubescens* tRNA^{Ser}_{CAG} sequence, both tRNAs can also be considered functional and unambiguously serylated. Assuming as much, leucines at CUG codons in *A. asiatica* must result from tRNA^{Leu}_{CAG}, which accordingly must be functional as well.

Although the evidence suggests the tRNA^{Ser}_{CAG} of *A. asiatica* must be functional (being such a strong resemblance to the functional species in *A. rubescens*), might the tRNA^{Leu}_{CAG} be misserylated? This seems highly unlikely, because the sequence contains all Leu-tRNA identity elements and is consistent with the Leu-tRNA consensus pattern, and the SerRS is highly specific for Ser-tRNAs, as evident from the unambiguous decoding of the five leucine codons (Data S2). Regardless, the *A. asiatica* tRNA^{Leu}_{CAG} must be a competitive decoding adaptor, because we found slightly more leucine than serine at CUG positions in all samples, although the ratio of tRNA^{Leu}_{CAG} to tRNA^{Ser}_{CAG} is 1 to 2.

Incidentally, tRNA^{Ser}_{CAG} from the *Ascoidea* clade yeasts are not related to tRNA^{Ser}_{CAG} from the DM clade. They belong to the tRNA^{Ser}_{GCU} family (for AGY codons), whereas the monophyletic tRNA^{Ser}_{CAG} are from the DM clade group within the HGA isoacceptors (Figure 2A). The AGA, CGA, and UGA isoacceptors (for UCU, UCG, and UCA codons, respectively) do not form monophyletic groups. Thus, the DM clade tRNA^{Ser}_{CAG} could have originated from any of these isoacceptors and not necessarily from a tRNA^{Ser}_{CGA} ancestor, as suggested by the few tRNA sequences available 20 years ago [13, 32].

Overall, the situation in *A. asiatica* rather resembles an experiment in *C. albicans*, where expression of a heterologous tRNA^{Leu}_{CAG} in wild-type background resulted in increased leucine incorporation at CUG sites in a reporter protein to 28% [21]. Similar to misaminoacylation, RNA-editing processes can also not explain the observed stochastic translation into both leucine and serine, even more so because it would require the editing of at least 2 nt to switch a CUG into a serine codon. Decoding of CUG by the tRNA^{Leu}_{UAG} isoacceptor through wobble base pairing could be responsible for some ambiguity (as seen in *A. rubescens* [0.83%] and the *Saccharomycopsis* species [0.38% and 1.48%]) but not for 50:50 stochasticity. Thus, all evidence suggests that CUG translation in *A. asiatica* is in fact the result of the presence of competing tRNA^{Ser}_{CAG} and tRNA^{Leu}_{CAG}. Definitive evidence would require detailed biochemistry of tRNA-amino acid association, but this is currently not tractable in this non-model species.

A. asiatica Copes with Stochastic Coding by Avoiding CUG in Key Locations

Ambiguous decoding is expected to be a very unstable intermediate state and to be resolved by loss of one of the tRNAs. To determine how *A. asiatica* copes with such a sub-optimal condition, we analyzed the positions of CUG codons in alignments of 26 proteins from 137 sequenced *Saccharomycotina* yeasts and 11 fungal outgroup species. First, *Ascoidea* species have considerably fewer CUG codons at conserved protein alignment positions than other yeasts with reassigned CUG: whereas both *B. inositolovora* and *C. lusitaniae* have discriminatory CUG codons at highly conserved serine positions, as has *N. peltata* at highly conserved alanine positions, all four *Ascoidea* clade yeasts lack CUG codons at highly conserved protein alignment positions (Figures 3 and S3). In *A. asiatica* in particular, none of the CUG codons fall at even moderately conserved alignment positions. This is not an effect of low codon usage, because all other leucine and serine codons show similar distributions on highly conserved alignment positions (Figures 3 and S3). Instead, this is likely to be the result of the stochastic codon translation selecting against CUG at positions of any importance (Figures 4A and 4B).

In contrast to the above, a low level of leucine (mis)incorporation at CUG positions does not select against CUG at conserved serine positions. DM clade species have similar numbers of CUG at conserved serine positions independent of having a potentially slightly misleucylated tRNA^{Ser}_{CAG} or having tRNA^{Ser}_{CAG} showing 100% serine identity due to the A37 antideterminant against LeuRS [33]. Unambiguous translation of CUG as serine both in *B. inositolovora* and in *C. lusitaniae* (Figure 1A; Table 1; Data S1) also suggests that the m¹G37 nucleotide, which was shown to

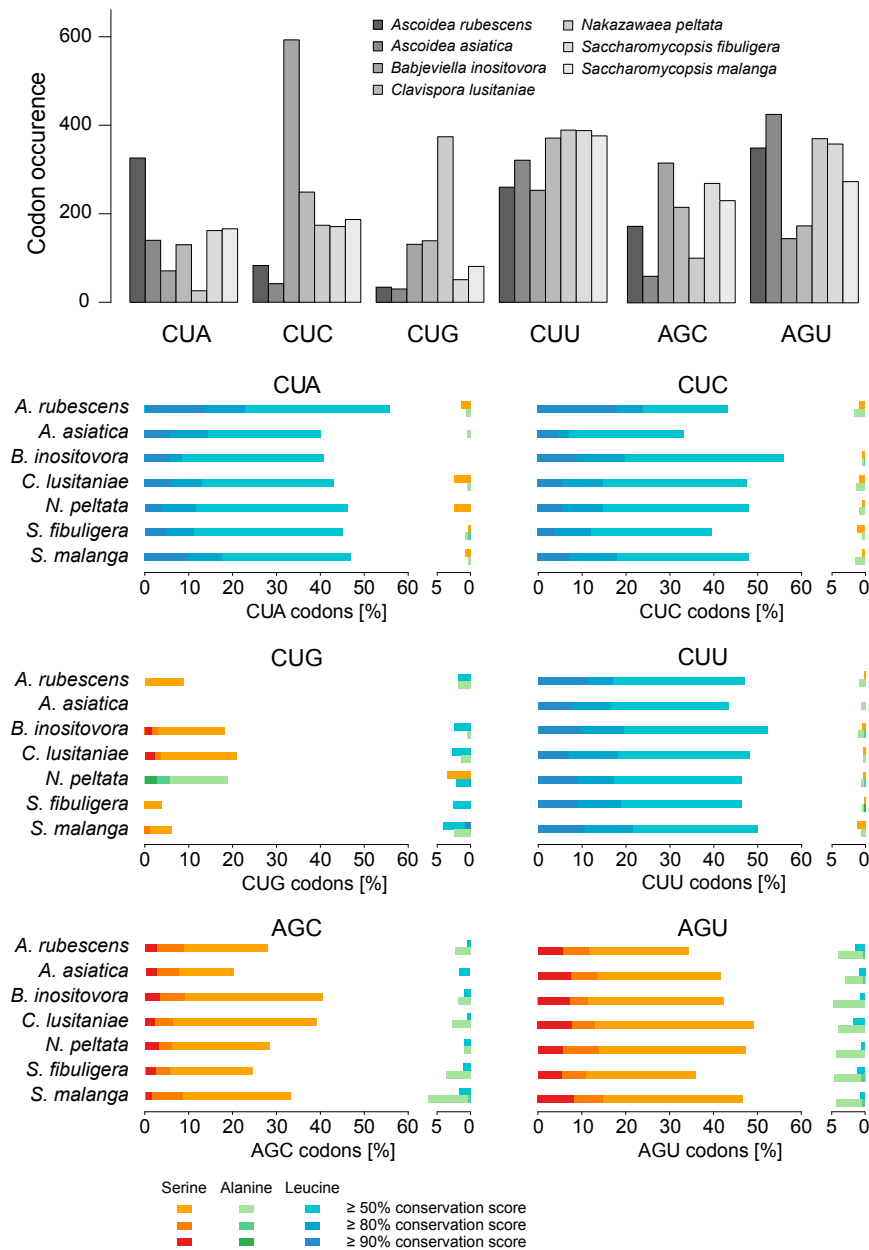


Figure 3. Conservation of the CUG Codon in Comparison to CUN and AGY Box Codons

The plot on top denotes the total number of CUN box and AGY box codons in the concatenated cytoskeletal and motor protein sequence alignment, whereas the plots below show the percentage of each codon present at alignment positions with a certain conservation score. On the left, codons found at alignment positions enriched in the expected amino acid are shown, contrasted by codons found at alignment positions enriched in an unexpected amino acid on the right. For the remaining leucine and serine codons, see also Figure S3.

used codon of the serine codon box, with the lowest level in *A. asiatica* (1.2%; 1.3% when considered part of the leucine codon box) and slightly higher levels in the other *Ascoidea* clade yeasts (2.4%–4.9%; Figure S4). In contrast, CUG codons are well established in *B. inositovora* (7.4%) and *C. lusitaniae* (10.6%), and the CUG codon in *N. peltata* is, with 27.5%, the second-most used alanine codon (Figure S4). In addition to this genome-wide reduction, effective CUG usage is further decreased by maintaining CUG codons in lowly expressed genes only as evidenced by the codon usage found in the proteomes. In the *A. asiatica* proteome, 0.4% of serine codons (0.2% with respect to leucine codons) are CUG codons, as are 0.6%–1.8% of the serine codons of the other *Ascoidea* clade yeasts (Figure S4). This suggests that *A. asiatica* has in part solved the problem of stochastic CUG translation by avoidance of the problem.

CUG Stochasticity Was Probably Resolved by Loss of Function of the $tRNA_{CAG}^{Leu}$ Gene in Other Species

How did *A. asiatica*'s closest relatives resolve codon ambiguity? To determine

cause minor-level misleucylation *in vitro* [20], might not have any effect on correct serylation *in vivo* because the *C. lusitaniae* $tRNA_{CAG}^{Ser}$ contains m¹G37 (Figure 2B). Also, there is no correlation of the number of CUGs at conserved serine positions with a free-living or pathogenic lifestyle of the *Candida* species [33]. Thus, it is considerably more likely that stochastic decoding can reduce or remove CUG from conserved positions whereas low-level mistranslation cannot.

Second, CUG codons are avoided in *A. asiatica* in general (Data S1) and, if used, used only in genes with very low to low expression levels (Figures 4C and 4D), both reducing the effective costs of stochastic encoding. In *Ascoidea* clade yeasts, CUG codons are genome-wide among the codons with lowest to third-lowest frequency. Accordingly, CUG is by far the least

the most likely position and timing of the divergence of the *Ascoidea* and *Saccharomycopsis* yeasts, we combined concatenation of multiple genes with deep taxonomic sampling (Figures 5 and S5). The resulting phylogenies strongly support monophyly of the *Ascoidea* clade yeasts and their branching before the split of the branch containing the DM clade and Pichiaceae species and the branch containing the Phaffomycetaceae, Saccharomycetaceae, and Saccharomycodaceae. Mapping the tRNA data onto the tree shows that the origin of the *Ascoidea* $tRNA_{CAG}^{Ser}$ dates back 190–230 Mya to the common origin of *Ascoidea* and *Saccharomycopsis*, whereas the $tRNA_{CAG}^{Leu}$ are divergent in *Ascoidea* and *Saccharomycopsis* and presumably appeared only after the split of these two branches (Figure S6). The *S. fibuligera* and *S. malanga* $tRNA_{CAG}^{Leu}$ are very similar, denoting

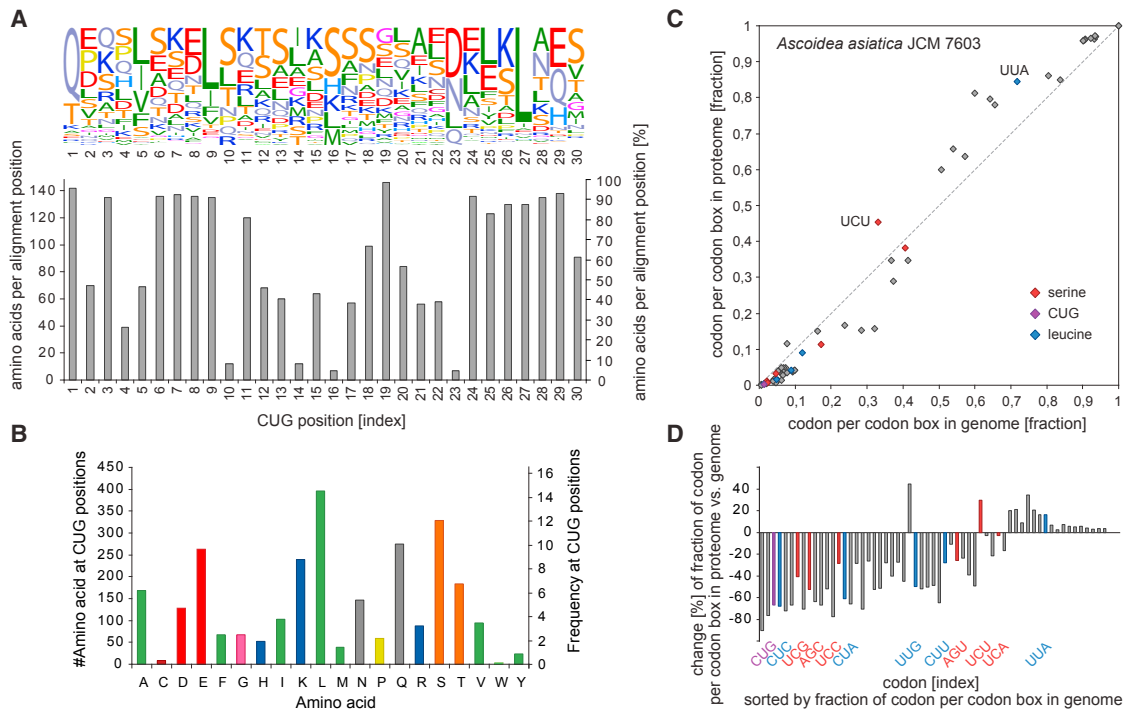


Figure 4. Amino Acid Composition at CUG Positions and Codon Usage in *A. asiatica*

(A) Amino acid composition at the 30 positions with *A. asiatica* CUG codons in the alignment of the cytoskeletal and motor proteins. The upper plot shows the amino acid frequency at each CUG codon position. For comparison, the number of sequences at each position contributing to the frequency plot is shown in the lower plot. The number of sequences never reaches 148 (100%) because some yeasts always miss one or the other gene. 14 of the 30 positions are at alignment positions present in the majority of the 148 species, whereas the other 16 positions are in loop regions of variable length or species- or clade-specific protein extensions. At these positions, only some yeast sequences are present.

(B) Global amino acid frequency over all 30 positions with CUG codons in *A. asiatica*.

(C) Codon usage in the genome versus proteome. The scatterplot presents the fraction of each codon per family box according to its usage in the genome, determined by analysis of the gene prediction dataset, versus its usage in the proteome, determined by analysis of the MS/MS data. Serine and leucine family box codons and the CUG codon are highlighted by red, blue, and purple color, respectively. The CUG codon is the leucine (and serine, respectively) codon least used. Serine and leucine codons preferably used in the proteome are indicated for orientation. See also Figure S4.

(D) Percentage difference between theoretical and actual codon usage. Proteins actually captured by LC-MS/MS show a preference/rejection of certain codons compared to their average usage in the genome. The CUG codon is among those found less often than expected, meaning that it is used more often in lowly than in highly expressed genes. Leucine and serine codons are highlighted the same as in (C).

a common origin in the ancient *Saccharomycopsis*. Given that these species predominantly translate CUG as serine, the ancient $\text{tRNA}_{\text{CAG}}^{\text{Leu}}$ was either non-functional in the first place already, or became non-functional after a period of codon ambiguity. If the ancient $\text{tRNA}_{\text{CAG}}^{\text{Leu}}$ was never functional, there would have been no constraint on reintroducing CUG codons at serine positions early. In this scenario, one would expect a considerable number of CUG codon positions to be shared between the two *Saccharomycopsis*, similar to the CUG position conservation seen in DM clade species (Figures 6 and S7) [33]. Such position conservation is, however, not found between the *Saccharomycopsis*, which in turn suggests that the ancestor of the *Saccharomycopsis* indeed experienced some time of codon ambiguity before its $\text{tRNA}_{\text{CAG}}^{\text{Leu}}$ became non-functional. Notably, the *Saccharomycopsis* $\text{tRNA}_{\text{CAG}}^{\text{Leu}}$ have purine nucleotides at position 20a in the D loop instead of the usual pyrimidine found in all yeast Leu-tRNAs including the *A. asiatica* $\text{tRNA}_{\text{CAG}}^{\text{Leu}}$ (Figure 2B). Such purine nucleotides have been shown to reduce leucylation efficiency in human tRNA^{Leu} by a factor of 25 while not changing their tRNA identity [24]. These data suggest that even if the *Sac-*

charomycopsis $\text{tRNA}_{\text{CAG}}^{\text{Leu}}$ are expressed at competitive levels, only a minor fraction is likely to be leucylated and functional. This is supported by analysis of RNA sequencing expression data for *S. fibuligera* under low and high glucose and sulfur limitation [16] showing the presence of the unprocessed (intron-containing) $\text{tRNA}_{\text{CAG}}^{\text{Ser}}$ and $\text{tRNA}_{\text{CAG}}^{\text{Leu}}$ in all conditions. For unknown reasons, these non-functional tRNAs were not disbanded already and are instead still kept in the genomes. In contrast, *A. rubescens* does not have a $\text{tRNA}_{\text{CAG}}^{\text{Leu}}$ and therefore has either never experienced codon ambiguity or has resolved it by a more recent loss of its $\text{tRNA}_{\text{CAG}}^{\text{Leu}}$. The absence of any CUG codons at highly conserved serine positions and the very low total number of CUG codons strongly support the second scenario. Future sequencing efforts redeeming the present undersampling might well reveal *Saccharomycopsis* species without $\text{tRNA}_{\text{CAG}}^{\text{Leu}}$ or *Ascoidea* relatives still containing a non-functional $\text{tRNA}_{\text{CAG}}^{\text{Leu}}$.

The findings in *A. asiatica*'s relatives render it most parsimonious that they experienced a phase of CUG stochasticity that was in turn resolved by loss of function of the $\text{tRNA}_{\text{CAG}}^{\text{Leu}}$ gene. Given the rate of introduction of CUGs at important positions in

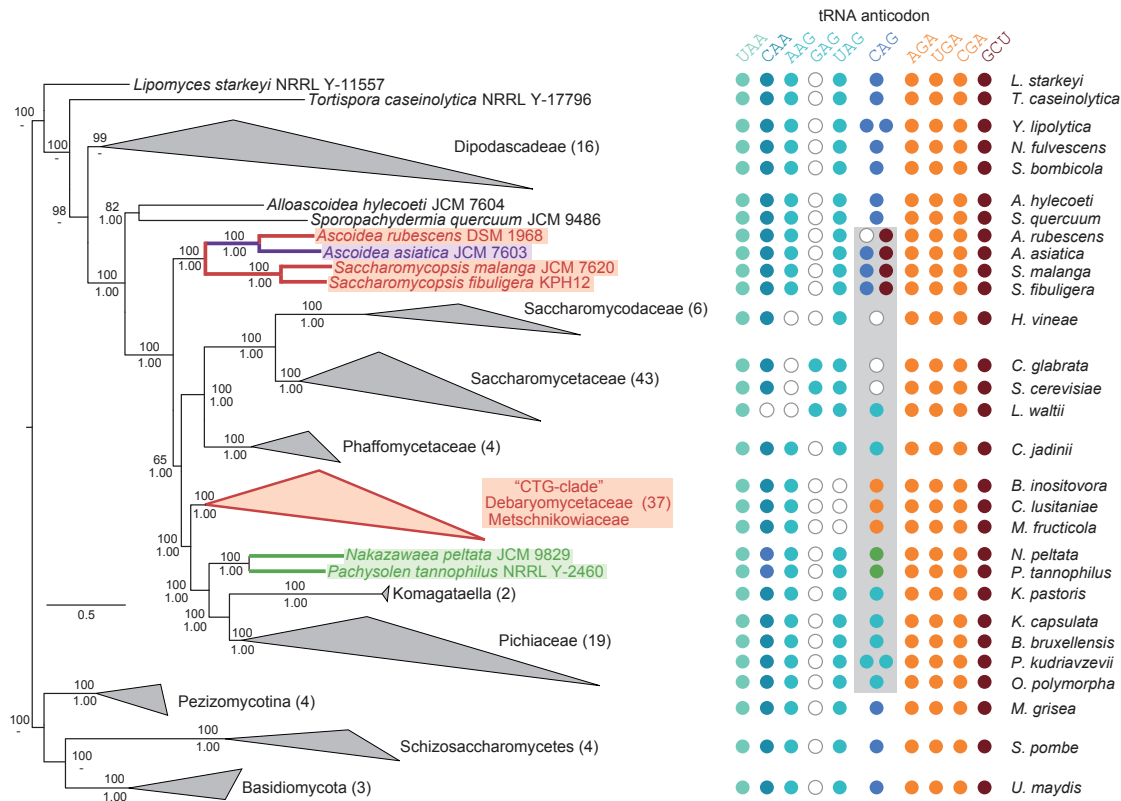


Figure 5. Yeast Phylogeny

RAXML-generated phylogeny of 137 yeast species and 11 fungal outgroup species. Support values for major branches are given as bootstrapping replicates (RAXML-generated tree, numbers above branches) and posterior probabilities (MrBayes-generated tree, numbers below branches). For display purposes, species of major lineages have been collapsed into groups, with the numbers in parentheses denoting the number of species and the corners of the triangles representing the shortest and longest distances within the groups. Species and groups employing alternative genetic codes are indicated by color: “CTG-clade” (DM clade) species *A. rubescens*, *S. malanga*, and *S. fibuligera* encode CUG as serine (red), *N. peltata* and *P. tannophilus* as alanine (green), and *A. asiatica* encodes CUG as both leucine and serine (purple). The grouping of the *Ascoidea* yeasts is consistent with a recent phylogenomics study [15]. Discrepancies with other published trees, which placed *Ascoidea* sister to the Phaffomycetaceae/Saccharomycetaceae/Saccharomycodaceae [34] or the Pichiaceae [17], are best explained by the deeper taxonomic sampling of early-branching yeasts (24 versus 10) in our study and the considerably increased sequence data (26 proteins versus 5), respectively. For each yeast, the presence (colored dots) and absence (white dots) of tRNA isoacceptors encoding the leucine (blue colors) and serine (red colors) codons are depicted at the side of the tree. For lineages collapsed in the tree, the tRNA repertoire of representative species is given. See also Figures S5 and S6.

the DM clade yeasts, the finding that only few CUGs are found at highly conserved serine positions in *Saccharomycopsis*, and none in *A. rubescens*, is most parsimonious, with the possibility that resolving codon ambiguity was a rather recent event in these species. Interestingly, both *A. rubescens* and the two *Saccharomycopsis* independently opted for the same tRNA, the one coding for serine. This is even more surprising, as it should be favorable to reestablish the complete leucine codon box and subsequently profit from simpler codon mutating schemes and decoding redundancy. A reason might be that in the case of 2-fold codon capture, the tRNA charged with the less deleterious amino acid (i.e., less important for protein stability) will be selected for.

Although it is suggestive that the solution seen in *A. asiatica* is an unstable solution and is generally deleterious and that *A. asiatica* is expected to also evolve to a position where it loses one of the two tRNAs in its evolutionary future, *A. asiatica* seems to have been living with stochastic translation for already 100 million years (Figure S6). Stochastic translation might have

been present in the ancestor of *Ascoidea* for an additional 100 million years before the split of *A. rubescens*. Thus, dramatically reducing the frequency of a certain codon and only using this codon in lowly expressed genes seems to be sufficient for a species to retain long-time viability. The growth rate of *A. asiatica* was similar to that of the other yeasts, indicating that the endogenous stochastic translation is not detrimental to *A. asiatica*'s fitness in rich medium. Although the evidence suggests that stochastic encoding is simply tolerated, whether there might be unusual circumstances where stochastic translation is beneficial is worthy of consideration.

DISCUSSION

Here we have shown that *A. asiatica* has an exceptional system in which the codon CUG is translated as either leucine or serine at high relative rates in a stochastic manner. A consequence of this is that the proteome is not deterministically predictable from the genome. This is tolerated by selection against CUG

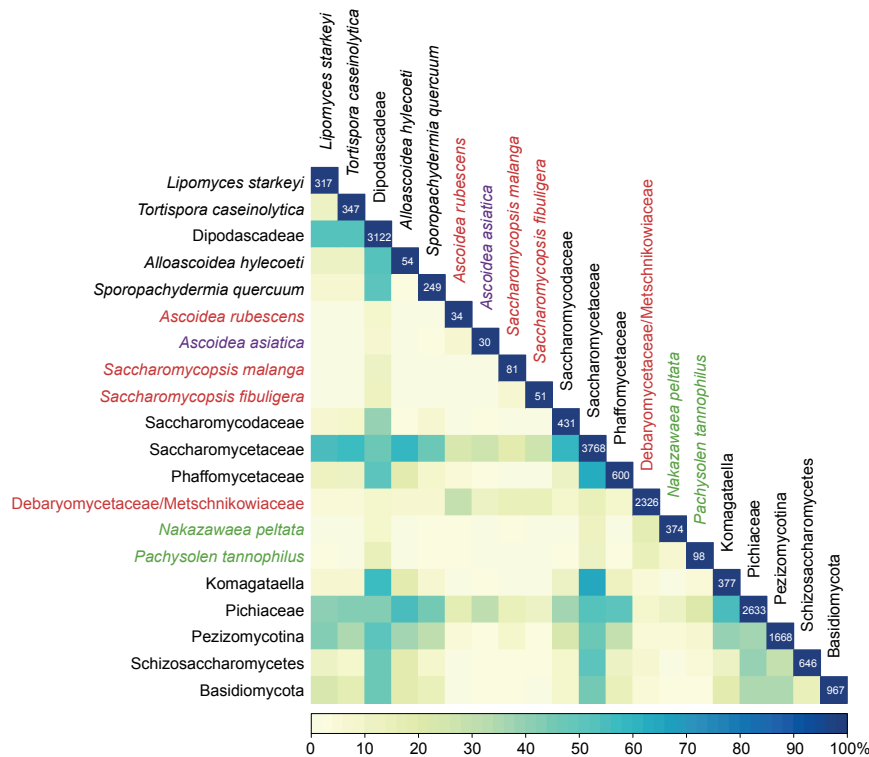


Figure 6. CUG Codon Position Conservation across Yeasts

The proportion of CUG codon positions in the concatenated cytoskeletal and motor protein sequence alignment shared between each two species or species groups. Proportions are calculated in relation to the number of CUG positions in the species or group with fewer CUG positions. Boxes on the diagonal represent the number of distinct CUG positions per species or species group. Given that CUG positions are present every 3.6th alignment position on average, there is remarkable clustering of the DM clade species and of species with CUG translated as leucine. In contrast, the *Ascoidea* yeasts share CUG positions only at background level, the level they share CUG positions with other yeasts. Notably, *P. tannophilus* and *N. peltata* do not share more CUG codon positions with each other than with any other yeast. This is consistent with their divergent tRNA^{Ala}_{CAG}, suggesting independent capture of the CUG codon. See also Figure S7.

generally, and especially at key locations and in highly expressed genes. The most parsimonious model to explain this supposes that the species has two functional tRNA species for the translation of CUG.

Are there any precedents? It has been reported that several nematodes encode leucine-type tRNAs with anticodons matching among others mainly glycine or isoleucine codons (together termed “nev-tRNAs”) [35], and that bacteria from the *Clostridia*, *Proteobacteria*, and *Acidobacteria* phyla contain novel types of tRNAs (termed “allo-tRNAs”), which are structurally similar to Sec-tRNA and have identity elements of Ser-tRNAs but contain anticodons corresponding to 35 distinct codons [22, 36]. *In vitro* aminoacylation experiments demonstrated that the nev-tRNAs are leucylated and that these tRNAs are able to decode GGG and AUA codons in translation assays [35]. However, whole-cell proteome analyses of *Caenorhabditis elegans* did not reveal detectable levels of leucines at GGG glycine codons, indicating that these nev-tRNAs are not used *in vivo* [37]. Similarly, multiple allo-tRNAs have been shown to be aminoacylated *in vitro* and to be used in translation in *E. coli*, but usage in their host organism has not been demonstrated yet [36]. Furthermore, although these allo-tRNAs suggest altered genetic codes in the respective hosts, genomic data demonstrating the presence or absence of standard cognate tRNAs are missing. Thus, these bacteria could have the genetic code strictly maintained or could employ alternative codes, and some might even show stochastic translation of one of the respective codons.

Our finding that stochastic translation is in general selected against but may still survive hundreds of millions of years in rare cases such as in *Ascoidea* clade species suggests that similar codon ambiguity might be present in other species as

well although not yet detected. Bacteria with allo-tRNAs might be the best candidates to look for and investigate potential further cases of stochastic translation. Other principally deleterious codon reassignments, such as the dual

decoding of stop codons, have also been found in independent species [9–11].

Do the new data fit into existing models of codon reassigment? At first glance, the situation found in *A. asiatica* seems to represent a prime example of the *ambiguous intermediate* hypothesis, according to which a new mutant tRNA appears and competes with the original cognate tRNA [38, 39]. This competition is thought to cause gradual codon frequency reduction and codon identity change followed by loss of the former cognate tRNA, and finally results in codon reassigment. One of the main ideas behind this scenario is that there should be faster evolutionary processes, such as selection, than genome-wide mutation and drift in codon frequency, which are the main causes for codon reassigment according to the *codon capture* hypothesis [40, 41]. However, considering the new findings about genetic codes in the *Ascoidea* clade, a global scenario for the entire yeast clade based on ambiguous intermediate states with competing tRNAs seems highly unlikely. First, at least six independent CUG capture events by completely different types of tRNAs with a combined probability of at most (1/64)⁶ would have to be considered (different types of tRNA^{Ser}_{CAG} in the DM clade and the *Ascoidea* clade, divergent tRNA^{Ala}_{CAG} in *Pachysolen* and *Nakazawaea*, and divergent tRNA^{Leu}_{CAG} in *Ascoidea* and *Saccharomycetaceae* branches, plus divergent tRNA^{Leu}_{CAG} in *Saccharomycetales*). Even if the tRNA^{Ala}_{CAG} and *Ascoidea* clade tRNA^{Leu}_{CAG} had been of common ancestry, there would have been still three independent ambiguous intermediate events (combined probability of (1/64)³). Second, the ambiguous intermediate scenario fails to explain the polyphyly of tRNA^{Leu}_{CAG} in *Saccharomycetales* and offers no apparent explanation for the complete absence of cognate tRNA^{Leu}_{CAG} in *Saccharomycodaceae* and

many Saccharomycetaceae [14]. Third, codon reassignments do not necessarily happen by fast, selection-driven processes, as evidenced by 100 million years of codon ambiguity in *A. asiatica* and up to 100 million years in the ancestors of the *Ascoidea* and the *Saccharomycopsis*. All these findings can, however, be well explained by the recently proposed *tRNA-loss-driven codon reassignment* hypothesis [14]. Indeed, both the further reassignments in independent yeast branches and the CUG capture by GCU-type Ser-tRNAs are predictions of this theory. According to this theory, the reassignments in yeasts originated from a single event, the loss of the original cognate tRNA^{Leu}_{CAG} before the split of the *Ascoidea* clade. The free codon could have subsequently been captured by any tRNA^{Leu}_{CAG}, tRNA^{Ser}_{CAG}, or tRNA^{Ala}_{CAG} (being the only tRNA species where the anticodon is not part of the aaRS recognition site). Although not considered when the theory was originally proposed, the tRNA-loss-driven codon reassignment scenario also allows for capture by two different tRNAs, as found in the *Ascoidea* clade. The *Saccharomycopsis* can thus be regarded as silenced cases of dual-codon capture, whereas *A. asiatica* is a frozen accident of dual-codon capture trapped in ambiguity for about 200 million years.

Previous examples of codons with dual and triple meanings were stop codons with the respective translation highly regulated and specified by codon context. Our finding of endogenous stochastic decoding by competing tRNAs provides the first example of a living species where the proteome cannot be deterministically predicted from the genome.

STAR★METHODS

Detailed methods are provided in the online version of this paper and include the following:

- KEY RESOURCES TABLE
- CONTACT FOR REAGENT AND RESOURCE SHARING
- METHOD DETAILS
 - Growth and lysis of yeast species
 - Growth and lysis of *Ascoidea rubescens*
 - Growth and lysis of *Ascoidea asiatica*
 - Genome assemblies and annotation
 - Mass spectrometry sequencing
 - Mass spectrometry analysis
 - tRNA gene identification and alignment
 - tRNA phylogeny
 - Generating the protein sequence alignment
 - Inferring species phylogeny
 - Calculating CUG position conservation
 - Conservation of leucine, serine and alanine alignment positions
- QUANTIFICATION AND STATISTICAL ANALYSIS
- DATA AND SOFTWARE AVAILABILITY

SUPPLEMENTAL INFORMATION

Supplemental Information includes seven figures and two data files and can be found with this article online at <https://doi.org/10.1016/j.cub.2018.04.085>.

A video abstract is available at <https://doi.org/10.1016/j.cub.2018.04.085#mmc5>.

ACKNOWLEDGMENTS

The authors would like to thank Rikiya Endoh, PhD, and the National BioResource Project (NBRP) program for generating the yeast genome assemblies and annotations and for permitting us to use the data prior to publication. In particular, we thank Rikiya Endoh for his comments on and careful reading of the manuscript. M.K. would like to thank Prof. Dr. Christian Griesinger for his continuous generous support. This work was supported by the European Research Council (advanced grant ERC-2014-ADG 669207 to L.D.H.) and the Medical Research Council (MR/L007215/1 to L.D.H.).

AUTHOR CONTRIBUTIONS

M.K. conceived the study. S.M. generated genome annotations and performed MS/MS data and phylogenetic analyses. H.D.S. prepared experimental samples. K.-T.P. and U.P. performed MS/MS experiments. H.U. supervised MS/MS analyses. L.D.H. was involved in data interpretation and manuscript writing. M.K. assembled and analyzed protein and tRNA sequences. S.M. and M.K. wrote the manuscript.

DECLARATION OF INTERESTS

The authors declare no competing interests.

Received: March 4, 2018

Revised: April 22, 2018

Accepted: April 24, 2018

Published: June 14, 2018

REFERENCES

1. Zaher, H.S., and Green, R. (2009). Fidelity at the molecular level: lessons from protein synthesis. *Cell* 136, 746–762.
2. Wohlgemuth, I., Pohl, C., Mittelstaet, J., Konevega, A.L., and Rodnina, M.V. (2011). Evolutionary optimization of speed and accuracy of decoding on the ribosome. *Philos. Trans. R. Soc. Lond. B Biol. Sci.* 366, 2979–2986.
3. Mohler, K., and Ibba, M. (2017). Translational fidelity and mistranslation in the cellular response to stress. *Nat. Microbiol.* 2, 17117.
4. Leinfelder, W., Zehelein, E., Mandrand-Berthelot, M.A., and Böck, A. (1988). Gene for a novel tRNA species that accepts L-serine and cotranslationally inserts selenocysteine. *Nature* 331, 723–725.
5. Metanis, N., and Hilvert, D. (2014). Natural and synthetic selenoproteins. *Curr. Opin. Chem. Biol.* 22, 27–34.
6. Keeling, P.J. (2016). Genomics: evolution of the genetic code. *Curr. Biol.* 26, R851–R853.
7. Kollmar, M., and Mülhhausen, S. (2017). Nuclear codon reassignments in the genomics era and mechanisms behind their evolution. *BioEssays*. Published online March 20, 2017. <https://doi.org/10.1002/bies.201600221>.
8. Turanov, A.A., Lobanov, A.V., Fomenko, D.E., Morrison, H.G., Sogin, M.L., Klobutcher, L.A., Hatfield, D.L., and Gladyshev, V.N. (2009). Genetic code supports targeted insertion of two amino acids by one codon. *Science* 323, 259–261.
9. Swart, E.C., Serra, V., Petroni, G., and Nowacki, M. (2016). Genetic codes with no dedicated stop codon: context-dependent translation termination. *Cell* 166, 691–702.
10. Heaphy, S.M., Mariotti, M., Gladyshev, V.N., Atkins, J.F., and Baranov, P.V. (2016). Novel ciliate genetic code variants including the reassignment of all three stop codons to sense codons in *Condylostoma magnum*. *Mol. Biol. Evol.* 33, 2885–2889.
11. Záhonová, K., Kostygov, A.Y., Ševčíková, T., Yurchenko, V., and Eliáš, M. (2016). An unprecedented non-canonical nuclear genetic code with all three termination codons reassigned as sense codons. *Curr. Biol.* 26, 2364–2369.

12. Kawaguchi, Y., Honda, H., Taniguchi-Morimura, J., and Iwasaki, S. (1989). The codon CUG is read as serine in an asporogenic yeast *Candida cylindracea*. *Nature* *341*, 164–166.
13. Miranda, I., Silva, R., and Santos, M.A.S. (2006). Evolution of the genetic code in yeasts. *Yeast* *23*, 203–213.
14. Mühlhausen, S., Findeisen, P., Plessmann, U., Urlaub, H., and Kollmar, M. (2016). A novel nuclear genetic code alteration in yeasts and the evolution of codon reassignment in eukaryotes. *Genome Res.* *26*, 945–955.
15. Riley, R., Haridas, S., Wolfe, K.H., Lopes, M.R., Hittinger, C.T., Göker, M., Salamov, A.A., Wisecaver, J.H., Long, T.M., Calvey, C.H., et al. (2016). Comparative genomics of biotechnologically important yeasts. *Proc. Natl. Acad. Sci. USA* *113*, 9882–9887.
16. Choo, J.H., Hong, C.P., Lim, J.Y., Seo, J.-A., Kim, Y.-S., Lee, D.W., Park, S.-G., Lee, G.W., Carroll, E., Lee, Y.-W., and Kang, H.A. (2016). Whole-genome de novo sequencing, combined with RNA-seq analysis, reveals unique genome and physiological features of the amylolytic yeast *Saccharomycopsis fibuligera* and its interspecies hybrid. *Biotechnol. Biofuels* *9*, 246.
17. Kurtzman, C.P., and Robnett, C.J. (2013). Relationships among genera of the Saccharomycotina (Ascomycota) from multigene phylogenetic analysis of type species. *FEMS Yeast Res.* *13*, 23–33.
18. Chi, Z., Chi, Z., Liu, G., Wang, F., Ju, L., and Zhang, T. (2009). *Saccharomycopsis fibuligera* and its applications in biotechnology. *Biotechnol. Adv.* *27*, 423–431.
19. Mühlhausen, S., and Kollmar, M. (2014). Predicting the fungal CUG codon translation with Bagheera. *BMC Genomics* *15*, 411.
20. Suzuki, T., Ueda, T., and Watanabe, K. (1997). The ‘polysemous’ codon—a codon with multiple amino acid assignment caused by dual specificity of tRNA identity. *EMBO J.* *16*, 1122–1134.
21. Gomes, A.C., Miranda, I., Silva, R.M., Moura, G.R., Thomas, B., Akoulitchev, A., and Santos, M.A.S. (2007). A genetic code alteration generates a proteome of high diversity in the human pathogen *Candida albicans*. *Genome Biol.* *8*, R206.
22. Mukai, T., Englert, M., Tripp, H.J., Miller, C., Ivanova, N.N., Rubin, E.M., Kyrpides, N.C., and Söll, D. (2016). Facile recoding of selenocysteine in nature. *Angew. Chem. Int. Ed. Engl.* *55*, 5337–5341.
23. Breitschopf, K., and Gross, H.J. (1994). The exchange of the discriminator base A73 for G is alone sufficient to convert human tRNA(Leu) into a serine-acceptor in vitro. *EMBO J.* *13*, 3166–3169.
24. Breitschopf, K., Achsel, T., Busch, K., and Gross, H.J. (1995). Identity elements of human tRNA(Leu): structural requirements for converting human tRNA(Ser) into a leucine acceptor in vitro. *Nucleic Acids Res.* *23*, 3633–3637.
25. Soma, A., Kumagai, R., Nishikawa, K., and Himeno, H. (1996). The anticodon loop is a major identity determinant of *Saccharomyces cerevisiae* tRNA(Leu). *J. Mol. Biol.* *263*, 707–714.
26. Yao, P., Zhu, B., Jaeger, S., Eriani, G., and Wang, E.-D. (2008). Recognition of tRNA(Leu) by *Aquifex aeolicus* leucyl-tRNA synthetase during the aminoacylation and editing steps. *Nucleic Acids Res.* *36*, 2728–2738.
27. Hou, Y.M., and Schimmel, P. (1988). A simple structural feature is a major determinant of the identity of a transfer RNA. *Nature* *333*, 140–145.
28. Hou, Y.M., and Schimmel, P. (1989). Evidence that a major determinant for the identity of a transfer RNA is conserved in evolution. *Biochemistry* *28*, 6800–6804.
29. Shi, J.P., Francklyn, C., Hill, K., and Schimmel, P. (1990). A nucleotide that enhances the charging of RNA minihelix sequence variants with alanine. *Biochemistry* *29*, 3621–3626.
30. Achsel, T., and Gross, H.J. (1993). Identity determinants of human tRNA(Ser): sequence elements necessary for serylation and maturation of a tRNA with a long extra arm. *EMBO J.* *12*, 3333–3338.
31. Normanly, J., Ollick, T., and Abelson, J. (1992). Eight base changes are sufficient to convert a leucine-inserting tRNA into a serine-inserting tRNA. *Proc. Natl. Acad. Sci. USA* *89*, 5680–5684.
32. Ueda, T., Suzuki, T., Yokogawa, T., Nishikawa, K., and Watanabe, K. (1994). Unique structure of new serine tRNAs responsible for decoding leucine codon CUG in various *Candida* species and their putative ancestral tRNA genes. *Biochimie* *76*, 1217–1222.
33. Mühlhausen, S., and Kollmar, M. (2014). Molecular phylogeny of sequenced Saccharomycetes reveals polyphyly of the alternative yeast codon usage. *Genome Biol. Evol.* *6*, 3222–3237.
34. Shen, X.-X., Zhou, X., Kominek, J., Kurtzman, C.P., Hittinger, C.T., and Rokas, A. (2016). Reconstructing the backbone of the Saccharomycotina yeast phylogeny using genome-scale data. *G3 (Bethesda)* *6*, 3927–3939.
35. Hamashima, K., Fujishima, K., Masuda, T., Sugahara, J., Tomita, M., and Kanai, A. (2012). Nematode-specific tRNAs that decode an alternative genetic code for leucine. *Nucleic Acids Res.* *40*, 3653–3662.
36. Mukai, T., Vargas-Rodriguez, O., Englert, M., Tripp, H.J., Ivanova, N.N., Rubin, E.M., Kyrpides, N.C., and Söll, D. (2017). Transfer RNAs with novel cloverleaf structures. *Nucleic Acids Res.* *45*, 2776–2785.
37. Hamashima, K., Mori, M., Andachi, Y., Tomita, M., Kohara, Y., and Kanai, A. (2015). Analysis of genetic code ambiguity arising from nematode-specific misacylated tRNAs. *PLoS ONE* *10*, e0116981.
38. Schultz, D.W., and Yarus, M. (1994). Transfer RNA mutation and the malleability of the genetic code. *J. Mol. Biol.* *235*, 1377–1380.
39. Schultz, D.W., and Yarus, M. (1996). On malleability in the genetic code. *J. Mol. Evol.* *42*, 597–601.
40. Osawa, S., and Jukes, T.H. (1989). Codon reassignment (codon capture) in evolution. *J. Mol. Evol.* *28*, 271–278.
41. Osawa, S., Jukes, T.H., Watanabe, K., and Muto, A. (1992). Recent evidence for evolution of the genetic code. *Microbiol. Rev.* *56*, 229–264.
42. Butler, G., Rasmussen, M.D., Lin, M.F., Santos, M.A.S., Sakthikumar, S., Munro, C.A., Rheinbay, E., Grabherr, M., Forche, A., Reedy, J.L., et al. (2009). Evolution of pathogenicity and sexual reproduction in eight *Candida* genomes. *Nature* *459*, 657–662.
43. Kersey, P.J., Allen, J.E., Armean, I., Boddu, S., Bolt, B.J., Carvalho-Silva, D., Christensen, M., Davis, P., Falin, L.J., Grabmueller, C., et al. (2016). *Ensembl Genomes 2016: more genomes, more complexity*. *Nucleic Acids Res.* *44* (D1), D574–D580.
44. Capra, J.A., and Singh, M. (2007). Predicting functionally important residues from sequence conservation. *Bioinformatics* *23*, 1875–1882.
45. Stanke, M., and Waack, S. (2003). Gene prediction with a hidden Markov model and a new intron submodel. *Bioinformatics* *19* (Suppl 2), ii215–ii225.
46. Cox, J., and Mann, M. (2008). MaxQuant enables high peptide identification rates, individualized p.p.b.-range mass accuracies and proteome-wide protein quantification. *Nat. Biotechnol.* *26*, 1367–1372.
47. Lowe, T.M., and Eddy, S.R. (1997). tRNAscan-SE: a program for improved detection of transfer RNA genes in genomic sequence. *Nucleic Acids Res.* *25*, 955–964.
48. Li, W., and Godzik, A. (2006). Cd-hit: a fast program for clustering and comparing large sets of protein or nucleotide sequences. *Bioinformatics* *22*, 1658–1659.
49. Stamatakis, A. (2014). RAxML version 8: a tool for phylogenetic analysis and post-analysis of large phylogenies. *Bioinformatics* *30*, 1312–1313.
50. Price, M.N., Dehal, P.S., and Arkin, A.P. (2010). FastTree 2—approximately maximum-likelihood trees for large alignments. *PLoS ONE* *5*, e9490.
51. Nguyen, L.-T., Schmidt, H.A., von Haeseler, A., and Minh, B.Q. (2015). IQ-TREE: a fast and effective stochastic algorithm for estimating maximum-likelihood phylogenies. *Mol. Biol. Evol.* *32*, 268–274.
52. Darriba, D., Taboada, G.L., Doallo, R., and Posada, D. (2012). jModelTest 2: more models, new heuristics and parallel computing. *Nat. Methods* *9*, 772.

53. Darriba, D., Taboada, G.L., Doallo, R., and Posada, D. (2011). ProtTest 3: fast selection of best-fit models of protein evolution. *Bioinformatics* *27*, 1164–1165.
54. Jow, H., Hudelot, C., Rattray, M., and Higgs, P.G. (2002). Bayesian phylogenetics using an RNA substitution model applied to early mammalian evolution. *Mol. Biol. Evol.* *19*, 1591–1601.
55. Ronquist, F., Teslenko, M., van der Mark, P., Ayres, D.L., Darling, A., Höhna, S., Larget, B., Liu, L., Suchard, M.A., and Huelsenbeck, J.P. (2012). MrBayes 3.2: efficient Bayesian phylogenetic inference and model choice across a large model space. *Syst. Biol.* *61*, 539–542.
56. Huson, D.H., and Bryant, D. (2006). Application of phylogenetic networks in evolutionary studies. *Mol. Biol. Evol.* *23*, 254–267.
57. Talavera, G., and Castresana, J. (2007). Improvement of phylogenies after removing divergent and ambiguously aligned blocks from protein sequence alignments. *Syst. Biol.* *56*, 564–577.
58. Smith, S.A., and O'Meara, B.C. (2012). treePL: divergence time estimation using penalized likelihood for large phylogenies. *Bioinformatics* *28*, 2689–2690.
59. Hatje, K., Hammesfahr, B., and Kollmar, M. (2013). WebScipio: reconstructing alternative splice variants of eukaryotic proteins. *Nucleic Acids Res.* *41*, W504–W509.
60. Shevchenko, A., Wilm, M., Vorm, O., Jensen, O.N., Podtelejnikov, A.V., Neubauer, G., Shevchenko, A., Mortensen, P., and Mann, M. (1996). A strategy for identifying gel-separated proteins in sequence databases by MS alone. *Biochem. Soc. Trans.* *24*, 893–896.
61. Oellerich, T., Bremes, V., Neumann, K., Bohnenberger, H., Dittmann, K., Hsiao, H.-H., Engelke, M., Schnyder, T., Batista, F.D., Urlaub, H., and Wienands, J. (2011). The B-cell antigen receptor signals through a preformed transducer module of SLP65 and CIN85. *EMBO J.* *30*, 3620–3634.
62. Beimforde, C., Feldberg, K., Nyländer, S., Rikkinen, J., Tuovila, H., Dörfelt, H., Gube, M., Jackson, D.J., Reitner, J., Seyfullah, L.J., and Schmidt, A.R. (2014). Estimating the Phanerozoic history of the Ascomycota lineages: combining fossil and molecular data. *Mol. Phylogenet. Evol.* *78*, 386–398.
63. Rambaut, A., and Drummond, A. (2016). FigTree v1.4.3. <http://tree.bio.ed.ac.uk/software/figtree/>.
64. Vizcaino, J.A., Csordas, A., del-Toro, N., Dienes, J.A., Griss, J., Lavidas, I., Mayer, G., Perez-Riverol, Y., Reisinger, F., Tement, T., et al. (2016). 2016 update of the PRIDE database and its related tools. *Nucleic Acids Res.* *44* (D1), D447–D456.

STAR★METHODS

KEY RESOURCES TABLE

REAGENT or RESOURCE	SOURCE	IDENTIFIER
Deposited Data		
<i>Ascoidea asiatica</i> NRRL Y-17576 genome assembly	NCBI	BCKQ01000001-BCKQ01000071
<i>Ascoidea rubescens</i> DSM 1968 genome assembly	NCBI [15]	LYBR01000001-LYBR01000326
<i>Babjeviella inositovora</i> NRRL Y-12698 genome assembly	NCBI [15]	LWKQ01000001-LWKQ01000211
<i>Clavispota lusitaniae</i> ATCC 42720 genome assembly	NCBI [42]	AAFT01000001-AAFT01000088
<i>Saccharomycopsis fibuligera</i> KPH12 genome assembly	NCBI [16]	CP012823-CP012829
<i>Saccharomycopsis malanga</i> NRRL Y-7175 genome assembly	NCBI	BCGJ01000001-BCGJ01000044
<i>Ascoidea asiatica</i> NRRL Y-17576 genome annotation	NBRP	N/A
<i>Ascoidea asiatica</i> NRRL Y-17576 genome annotation	This paper	N/A
<i>Ascoidea rubescens</i> DSM 1968 genome annotation	Ensembl Fungi [43]	N/A
<i>Babjeviella inositovora</i> NRRL Y-12698 genome annotation	Ensembl Fungi [43]	N/A
<i>Clavispota lusitaniae</i> ATCC 42720 genome annotation	Ensembl Fungi [43]	N/A
<i>Nakazawaea peltata</i> NRRL Y-6888 genome annotation	NBRP	N/A
<i>Saccharomycopsis fibuligera</i> KPH12 genome annotation	This paper	N/A
<i>Saccharomycopsis malanga</i> NRRL Y-7175 genome annotation	NBRP	N/A
tRNA identification	[14]; This paper	N/A
Sequence data	Figshare [33]; This paper	https://doi.org/10.6084/m9.figshare.6086639
Phylogenetic trees	Figshare; This paper	https://doi.org/10.6084/m9.figshare.6086639
Mass spectrometry data	ProteomeXchange via PRIDE [44]	PXD009494
Experimental Models: Organisms/Strains		
<i>Ascoidea asiatica</i>	NRRL	Y-17576
<i>Ascoidea rubescens</i>	DSMZ	1968
<i>Babjeviella inositovora</i>	NRRL	Y-12698
<i>Clavispota lusitaniae</i>	NRRL	Y-11827
<i>Nakazawaea peltata</i>	NRRL	Y-6888
<i>Saccharomycopsis fibuligera</i>	NRRL	Y-2388
<i>Saccharomycopsis malanga</i>	NRRL	Y-7175
Software and Algorithms		
Custom scripts for data generation and parsing	[14]; This paper	N/A
Gene prediction	AUGUSTUS [45]	http://bioinf.uni-greifswald.de/augustus/binaries/
Mass spectrometry analysis and search	MaxQuant [46]	http://www.coxdocs.org/doku.php?id=maxquant:common:download_and_installation
tRNA identification	tRNAscan [47]	http://lowelab.ucsc.edu/tRNAscan-SE/
Alignment redundancy reduction	CD-HIT [48]	http://weizhongli-lab.org/cd-hit/
Maximum likelihood tree calculation	RAxML v8.2.10 [49]	https://github.com/stamatak/standard-RAxML

(Continued on next page)

Continued

REAGENT or RESOURCE	SOURCE	IDENTIFIER
Maximum likelihood tree calculation	FastTree v2.1.9 [50]	http://www.microbesonline.org/fasttree/#Install
Maximum likelihood tree calculation	IQ-TREE v1.63b [51]	https://github.com/Cibiv/IQ-TREE
Scoring of substitution models for (tRNA) ML-tree generation	jModelTest v2.1.10 [52]	https://github.com/ddarriba/jmodeltest2
Scoring of substitution models for (protein) ML-tree generation	ProtTest v3.4.2 [53]	https://github.com/ddarriba/prottest3
Bayesian tree calculation (tRNA)	Phase v3.0 [54]	https://github.com/james-monkeyshines/rna-phase-3
Bayesian tree calculation (protein)	MrBayes v3.2.6 [55]	http://mrbayes.sourceforge.net/download.php
Phylogenetic network calculation	SplitsTree v4.14.4 [56]	http://ab.inf.uni-tuebingen.de/data/software/splitree4/download/welcome.html
Alignment position reduction	Gblocks v0.91b [57]	http://molevol.cmima.csic.es/castresana/Gblocks.html
Divergence time estimation	treePL [58]	https://github.com/blackrim/treePL
Tree visualization	FigTree v1.4.3 (Rambaut and Drummond)	http://tree.bio.ed.ac.uk/software/figtree/
Gene structure reconstruction	WebScipio [59]	http://www.webscipio.org/
Alignment position conservation calculation	conservation code toolbox [44]	http://compbio.cs.princeton.edu/conservation/

CONTACT FOR REAGENT AND RESOURCE SHARING

Further information and requests for resources and reagents should be directed to and will be fulfilled by the Lead Contact, Martin Kollmar (mako@nmr.mpibpc.mpg.de).

METHOD DETAILS

Growth and lysis of yeast species

Babjeviella inositovora NRRL Y-12698, *Clavispora lusitaniae* NRRL Y-11827 (CBS 6936), *Nakazawaea peltata* NRRL Y-6888, *Saccharomycopsis fibuligera* NRRL Y-2388 (ATCC 36309) and *Saccharomycopsis malanga* NRRL Y-7175 were obtained from the Agricultural Research Service (ARS) Culture Collection Database (NRRL - Northern Regional Research Laboratory). *C. lusitaniae* was grown in YEPD medium (containing [% w/v]: bacto peptone 2.0; yeast extract 1.0; glucose 2.0) at 25°C. *B. inositovora*, *N. peltata* and *S. malanga* were grown in YM medium (NRRL Medium No. 6, containing [% w/v]: yeast extract 0.3; malt extract 0.3; peptone 0.5; glucose 1.0) at 25°C. *S. fibuligera* samples were grown in YM medium (sample [1]) and malt extract medium (sample [2]; ATCC Medium 325 [Blakeslee's formula; % w/v]: malt extract 2.0; glucose 2.0; peptone 1.0) at 25°C. Cells were harvested by centrifugation (5' at 4,400 x g), and washed with water. Aliquots of cells were lysed in 2 M NaOH and 5% mercaptoethanol, and proteins precipitated with 10% trichloroacetic acid (TCA) (both steps with 10 min incubation on ice). For neutralizing, the pellet was rinsed once with 1.5 M TRIS-base and proteins were resuspended in SDS sample buffer. Proteins were resolved on 4%–12% SDS-PAGE.

Growth and lysis of *Ascoidea rubescens*

Ascoidea rubescens DSM 1968 (= NRRL Y-17699) was obtained from the German Collection of Microorganisms and Cell Cultures (DSMZ - Deutsche Sammlung von Mikroorganismen und Zellkulturen). Cells were grown in malt-soya peptone medium (containing [% w/v]: malt extract 3.0, soya peptone 0.3) at 22°C. Clusters of *A. rubescens* cells were recovered using a loop. After washing with water cells were ground in liquid nitrogen. Sample buffer was added to the extract and the suspension was collected and fractionated by SDS-PAGE.

Growth and lysis of *Ascoidea asiatica*

Ascoidea asiatica NRRL Y-17576 was obtained from the Agricultural Research Service (ARS) Culture Collection Database (NRRL - Northern Regional Research Laboratory) and grown in malt-soya peptone medium (sample [1]), malt extract medium (samples [2] and [4]), and YM (sample [3]) at 22°C. *A. asiatica* cells from sample [1] were collected by centrifugation and washed. After washing with water cells were ground in liquid nitrogen. Cells from samples [2] to [4] were harvested by centrifugation (5' at 4,400 x g), and washed with water. Aliquots of cells were lysed in 2 M NaOH and 5% mercaptoethanol, and proteins precipitated with 10% trichloroacetic acid (TCA) (both steps with 10 min incubation on ice). For neutralizing, the pellet was rinsed once with 1.5 M TRIS-base. Sample buffer was added to the extracts and the suspensions were collected and fractionated by SDS-PAGE.

Genome assemblies and annotation

All genome assemblies were obtained from NCBI with the following GenBank accessions: *Ascoidea asiatica* NRRL Y-17576: BCKQ01000001-BCKQ01000071; *Ascoidea rubescens* DSM 1968: LYBR01000001-LYBR01000326 [15], *Babjeviella inositovora* NRRL Y-12698: LWKQ01000001-LWKQ01000211 [15]; *Clavispora lusitaniae* ATCC 42720: AAFT01000001-AAFT01000088 [42]; *Saccharomycopsis fibuligera* KPH12: CP012823-CP012829 [16]; and *Saccharomycopsis malanga* NRRL Y-7175: BCGJ01000001-BCGJ01000044. Genome annotations for *Ascoidea rubescens* DSM 1968 [15], *Babjeviella inositovora* NRRL Y-12698 [15] and *Clavispora lusitaniae* ATCC 42720 [42] were obtained from Ensembl Fungi [43]. The genome annotations for *Ascoidea asiatica* NRRL Y-17576, *Nakazawaea peltata* NRRL Y-6888 and *Saccharomycopsis malanga* NRRL Y-7175 were obtained from the National BioResource Project (NBRP) program web page (http://www.jcm.riken.jp/cgi-bin/nbrp/nbrp_list.cgi). *Ascoidea asiatica* NRRL Y-17576 and *Saccharomycopsis fibuligera* KPH12 genes were predicted with AUGUSTUS [45] using the parameter “genemodel=complete,” the gene feature set of *Candida albicans*, and the standard codon translation table.

Mass spectrometry sequencing

SDS-PAGE-separated protein samples were processed as described by Shevchenko et al. [60]. The resuspended peptides in sample loading buffer (2% acetonitrile and 0.05% trifluoroacetic acid) were separated and analyzed by an Ultimate 3000 RSLCnano HPLC system (Thermo Fisher Scientific) coupled online to a Q Exactive HF or a Q Exactive Plus mass spectrometer (Thermo Fisher Scientific). First, the peptides were desalted on a reverse phase C18 pre-column (Dionex 5 mm long, 0.3 mm inner diameter) for 3 min. After 3 min the precolumn was switched online with the analytical column (30 cm long, 75 μ m inner diameter) prepared in-house using ReproSil-Pur C18 AQ 1.9 μ m reversed phase resin (Dr. Maisch GmbH). The peptides were separated with a linear gradient of 5%–35% buffer (80% acetonitrile and 0.1% formic acid) at a flow rate of 300 nL/min (with back pressure 500 bars) over 88 min gradient time. The pre-column and the column temperature were maintained at 50°C. In the Q Exactive Plus the MS data were acquired by scanning the precursors in mass range from 350 to 1600 m/z at a resolution of 70,000 at m/z 200. Top 20 precursor ions were chosen for MS2 by using data-dependent acquisition (DDA) mode at a resolution of 17,500 at m/z 200 with maximum IT of 50 ms. In the Q Exactive HF the MS data were acquired by scanning the precursors in mass range from 350 to 1600 m/z at a resolution of 60,000 at m/z 200. Top 30 precursor ions were chosen for MS2 by DDA mode at a resolution of 15,000 at m/z 200 with maximum IT of 50 ms. Data for *Ascoidea asiatica*, *Saccharomyces fibuligera* and *Ascoidea rubescens* were measured on Q Exactive Plus instrument. All other Data were measured on Q Exactive HF instrument.

Mass spectrometry analysis

Data analysis and search were performed using MaxQuant v.1.5.2.8 [46] as search engine with 1% FDR. To obtain peptide mappings free of CUG-translation bias, 20 replicates for each genome annotation were generated with the CUG codon translated as different amino acid in each replicate. To reduce database size and redundancy, predicted proteins were split at lysine and arginine residues into peptides resembling trypsin proteolysis. Peptides containing CUG codons were fused together with the two subsequent peptides so that CUG-containing fragments can be detected with up to two missed cleavages. The remaining peptides were fused back together as long as they formed consecutive blocks. By this process we could reduce database size and redundancy by 31%–89% depending on CUG-usage in the respective coding sequences. Search parameters for searching the precursor and fragment ion masses against the databases were as described in Oellerich et al. [61] except that all peptides shorter than seven amino acids were excluded. The datasets were searched with the gene prediction dataset for the respective species, except for the second sample [2] of *A. asiatica* that was searched with both the gene prediction dataset from NBRP [= 2A] and the newly generated AUGUSTUS gene prediction dataset [= 2B]. To claim CUG codon translations with high confidence, we determined CUG positions with b- and y-type fragment ions at both sides that allow for determining the amino acids' mass. Only those positions were regarded as fully supported by the data. In addition, we regard the first two amino acids as combinedly fully supported if a b- and/or y-type fragment ion exists for the C-terminal site of this di-peptide and the combined mass of the two amino acids is unambiguous.

tRNA gene identification and alignment

tRNA genes from 60 Saccharomycetes and four Schizosaccharomycetes were taken from a previous analysis [14]. tRNA genes for additional 77 Saccharomycetes sequenced since then were identified with tRNAscan [47] using standard parameters. The tRNAs from the 60 Saccharomycetes and four Schizosaccharomycetes were sorted by anticodon. From the newly sequenced yeasts, only the tRNAs with CAG anticodon were extracted from the predictions and added to the other tRNA_{CAG}. The tRNAs from each anticodon group were aligned and mitochondrial tRNAs, fragmented tRNAs and obviously unusual tRNAs were removed manually. To generate a dataset with a broad and unbiased sampling of as many tRNA types as possible, redundancy for all anticodon groups but CAG was reduced to 90% sequence identity by applying the CD-HIT suite [48]. The CAG anticodon group was first split into leucine-, serine, and alanine-encoding tRNAs and then reduced to 95% sequence identity.

To prepare a representative tRNA dataset for tRNA-type determination, all tRNA_{CAG} from the reduced alignments, the first six tRNAs from each leucine, serine, alanine, valine, phenylalanine, asparagine and methionine anticodon alignment, and the first six tRNAs from tRNA_{CAG} the AGU threonine anticodon alignment were combined.

tRNA phylogeny

tRNA phylogenies were inferred using maximum likelihood, Bayesian and split networks methods. 1) Maximum likelihood trees were computed with RAxML v8.2.10 [49], FastTree v2.1.9 [50], and IQ-TREE v1.63b [51]. First, a substitution model was selected using jModelTest v2.1.10 [52]. jModelTest found the GTR +G +I model to be the best under the AICc framework followed by GTR +G as second best model. RAxML was run with substitution model GTR +G +I and 1,000 bootstrap replicates. FastTree does not allow to control for proportion of invariable sites, and was therefore started with the second best substitution model, GTR +G. IQ-Tree was run with the model selected by its build-in ModelSelector according to BIC (Ala-tRNA alignment: TIME+G4; Ser-tRNA alignment: TVMe+I+G4; Leu-tRNA alignment: TPM2u+I+G4; alignment of representative tRNAs: TVM+R5). To assess branch support, the analyses were performed with 1,000 bootstrap replicates. 2) Bayesian trees were inferred using Phase v3.0 [54] and MrBayes v3.2.6 [55]. Phase was started with a mixed model consisting of REV +G for loops and RNA7D +G for stem regions as suggested by the developers in their example control files. 750,000 burn-in cycles and 1,500,000 sampling cycles with a sampling period of 150 cycles have been performed. Met-tRNAs were defined to form a monophyletic cluster. MrBayes was started with the 4by4 option, two independent runs with 1,000,000 generations, four chains, and a random starting tree. Trees were sampled every 1,000th generation and the first 25% of the trees were discarded as “burn-in” before generating a consensus tree. A separate run was performed with structural information and a partitioned model with option 4by4 for loop regions and doublet for stem regions. 3) An unrooted phylogenetic network was computed using SplitsTree v4.14.4 [56] with the neighbor-net method and 1,000 bootstrap replicates.

Generating the protein sequence alignment

The protein sequences of the actin and actin-related, CapZ, dynein heavy chain, kinesin, myosin and tubulin proteins of 81 yeasts, four Pezizomycotina and three Basidiomycota were added to the already existing multiple sequence alignments from 60 yeast species following the previously described approach [33]. A 148-taxa, 26-protein supermatrix was then constructed for further analysis, resulting in an alignment of 35,202 columns. A reduced alignment was generated using Gblocks v0.91b [57] with parameters allowing less stringent block selection (smaller final blocks, gap positions within the final blocks, less strict flanking positions). Gblocks reduced the alignment to 7,942 amino acid positions in 385 blocks.

Inferring species phylogeny

Phylogenetic trees were generated on both the full and the gblocks-reduced alignments using two different methods: 1) Bayesian trees were inferred using MrBayes v3.2.6 [55] with the mixed amino acid option, two independent runs with 1,000,000 generations, four chains, and a random starting tree. 2) Maximum likelihood trees were inferred with RAxML v8.2.10 [49] and IQ-TREE v1.63b [51]. RAxML was run with substitution model LG +G +I, which was the best-fitting model according to the Bayesian information criterion (BIC) determined by ProtTest v3.4.2 [53], and 1,000 bootstrap replicates. IQ-Tree was run with the model selected by its build-in ModelSelector according to BIC, LG +F +R12 for the full alignment and LG +F +R11 for the gblocks-reduced alignment. To assess branch support, the analyses were performed with 1,000 bootstrap replicates. Both ML methods gave effectively identical results, as did gblocks-reduced and full alignments, indicating that the results are not software specific. The divergence times of species were estimated with the penalized-likelihood approach as implemented in treePL [58] based on the RAxML-generated tree of the full alignment. The splits between *Saccharomyces cerevisiae* and *Candida albicans*, and *C. albicans* and *Neurospora crassa* [62] were constrained simultaneously. All phylogenetic trees were visualized using FigTree v1.4.3 [63].

Calculating CUG position conservation

Gene structures of the assembled protein sequences were reconstructed with WebScipio [59], and the structures of all “complete” genes (e.g., genes that do not contain a sequence shift) were mapped onto the concatenated protein sequence alignment allowing any kind of codon-based comparisons. Overall, the mapped genes contain 34,517 CTG codons that distribute to 9,857 alignment positions.

Conservation of leucine, serine and alanine alignment positions

Conservation scores were calculated for all alignment positions containing leucine, serine or alanine with the conservation code toolbox [44], a window size of 3 and the property entropy as conservation estimation method. Alignment blocks of 15 positions before and after the respective position of interest were generated to reduce any further influence of the rest of the alignment on the scoring process. Sequences with CUG codons in the block have been retained. Any stop codons present in the concatenated alignment have been replaced by ‘X’ for calculating scores.

QUANTIFICATION AND STATISTICAL ANALYSIS

Binomial test was implemented using R function `binom.test`, with $p = 0.5$ and employing a two sided test.

DATA AND SOFTWARE AVAILABILITY

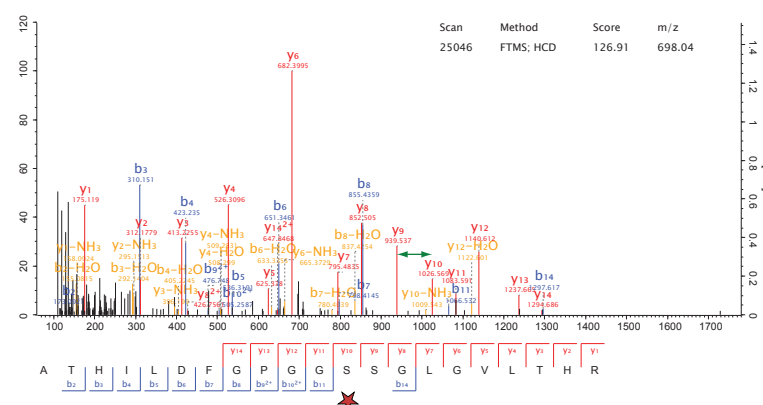
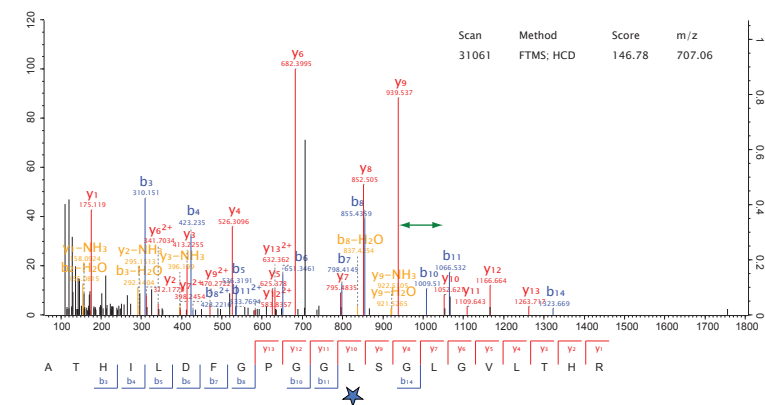
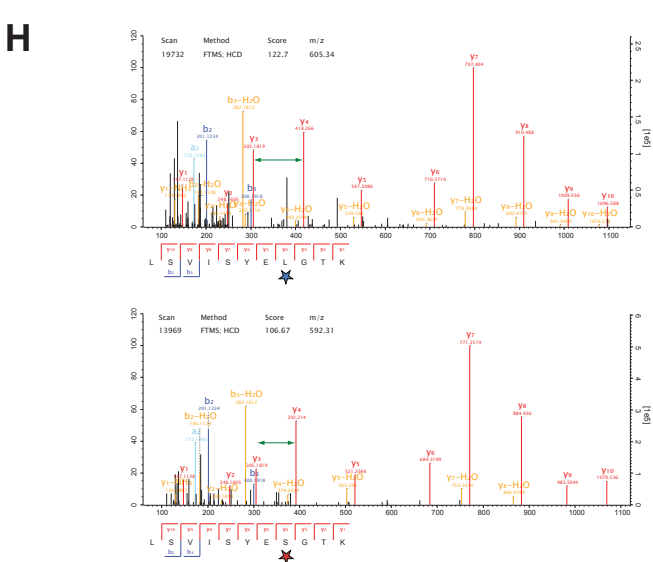
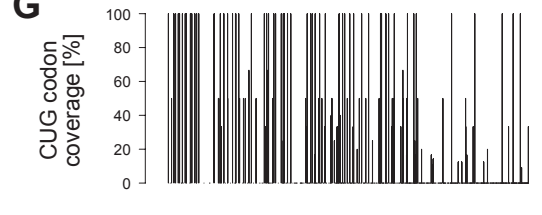
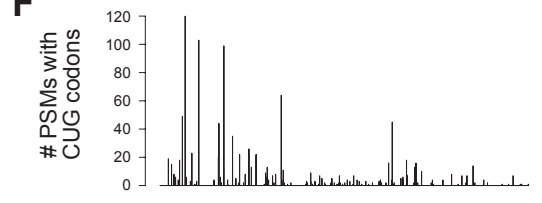
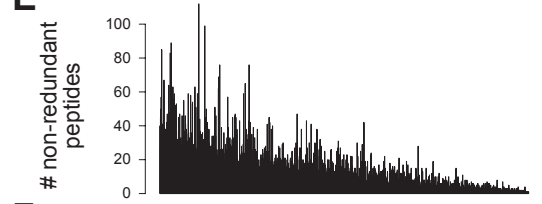
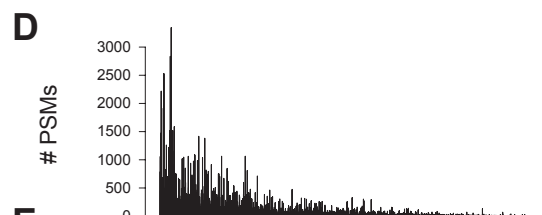
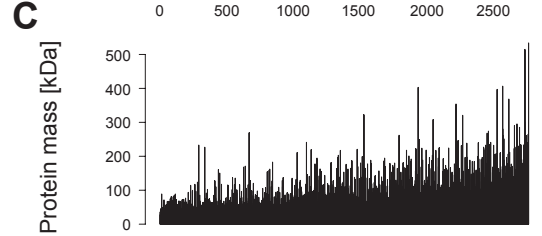
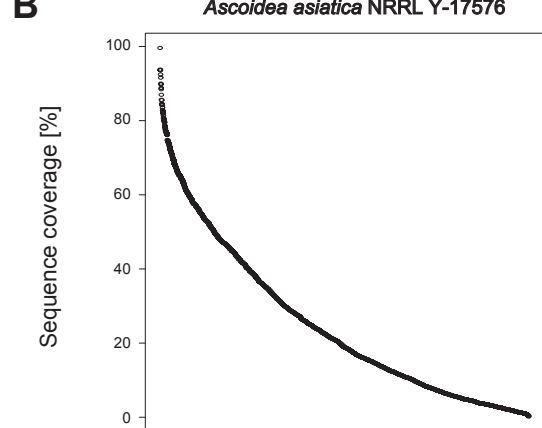
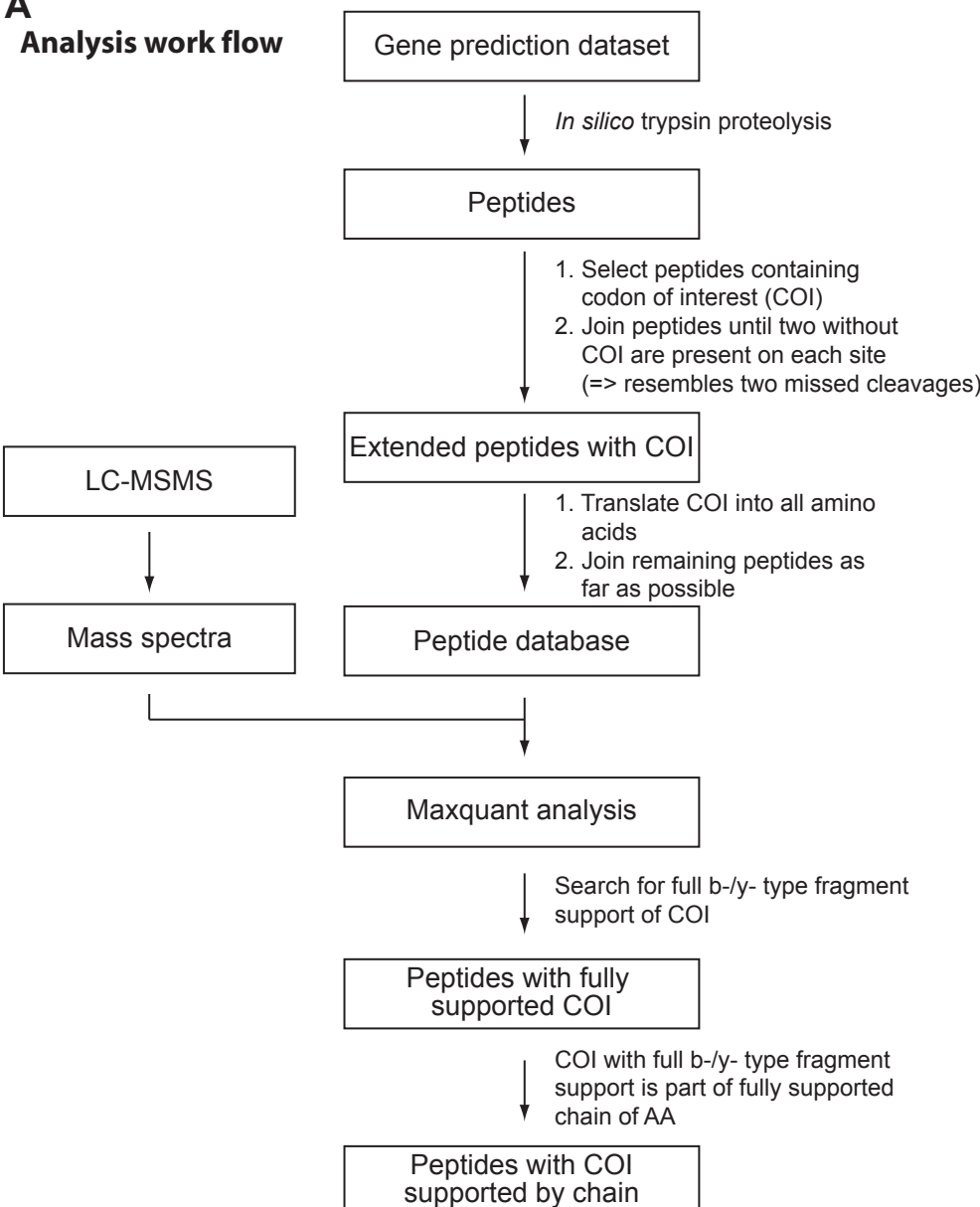
The mass spectrometry data from this study have been submitted to the ProteomeXchange Consortium (<http://proteomecentral.proteomexchange.org>) via the PRIDE [64] partner repository with the dataset identifier PXD009494. Sequence data and phylogenetic trees are available from Figshare (<https://doi.org/10.6084/m9.figshare.6086639>).

Current Biology, Volume 28

Supplemental Information

**Endogenous Stochastic Decoding
of the CUG Codon by Competing
Ser- and Leu-tRNAs in *Ascoidea asiatica***

Stefanie Mühlhausen, Hans Dieter Schmitt, Kuan-Ting Pan, Uwe Plessmann, Henning Urlaub, Laurence D. Hurst, and Martin Kollmar

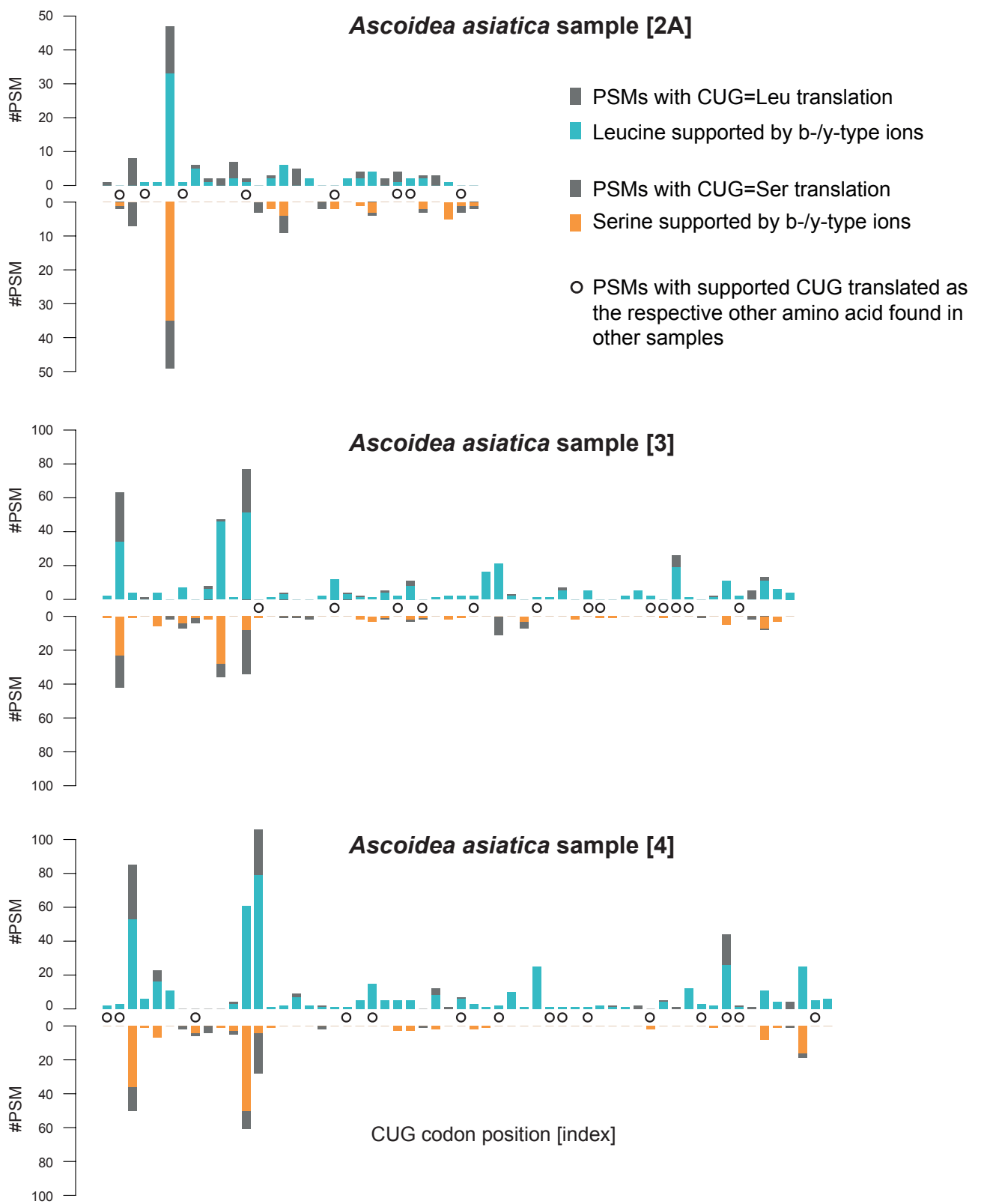


Gene index

Figure S1. Summary of the proteome analysis workflow and statistics, Related to Figure 1.

A) For the database search we generated gene prediction datasets, in which all codons were iteratively translated into all amino acids. The peptides with differently translated codons have distinct total MW, accordingly different precursor ion masses and result in different spectra. B) Distribution of sequence coverage of identified proteins. C) Molecular weight of the respective proteins. D) Number of peptides matching to the respective protein. E) Number of non-redundant peptides matching to the respective protein. F) Number of peptide spectrum matches (PSMs) covering CUG-codon positions. G) Percentage of the CUG-codon positions per protein covered by the proteomics data. H) Representative LC-MS/MS spectra featuring CUG codons translated as serine and leucine (marked with stars).

A



B

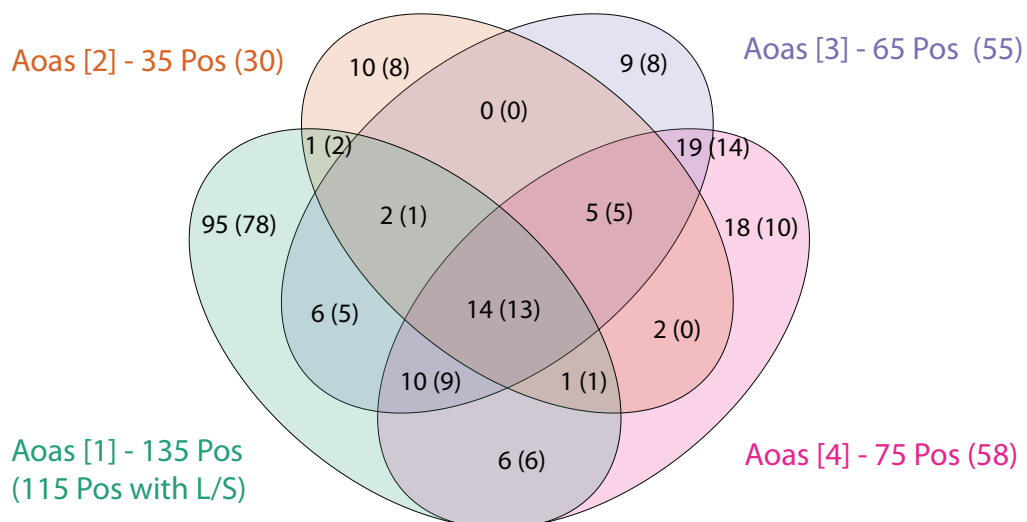


Figure S2. Peptides with CUG codon positions found in *Ascoidea asiatica* samples [2A], [3] and [4], which were grown in different media, Related to Figure 1B.

A) Gray bars denote the number of total PSMs covering a certain CUG position. These PSMs include those without support by b-/y-type ions. The PSMs with CUG positions supported by b-/y-type ions were colored: Blue bars represent PSMs with CUG translated as leucine and orange bars denote PSMs with CUG translated as serine. CUG positions exclusively translated with other amino acids than leucine or serine have been omitted. B) Overlap of supported CUG codon positions covered in different samples. Aoas [1] corresponds to the sample described in the main text, Aoas [2A], Aoas [3] and Aoas [4] denote further samples grown in different media. The numbers denote the total numbers of PSMs covering CUG codon positions including those not supported by b-/y-type fragment ions. For comparison, the numbers of CUG codons found with ambiguous translation (leucine or serine and, additionally, another amino acid) are given. CUG codon positions covered in multiple samples and translated by other amino acids indicate genome sequencing errors or differences between sequenced and analysed strain. This is true for one of the CUG codon positions covered by all four samples, and two positions covered by three samples. The majority of b-/y-type ion supported positions (95-99%) is, however, only translated by serine and leucine (see also Data S1).

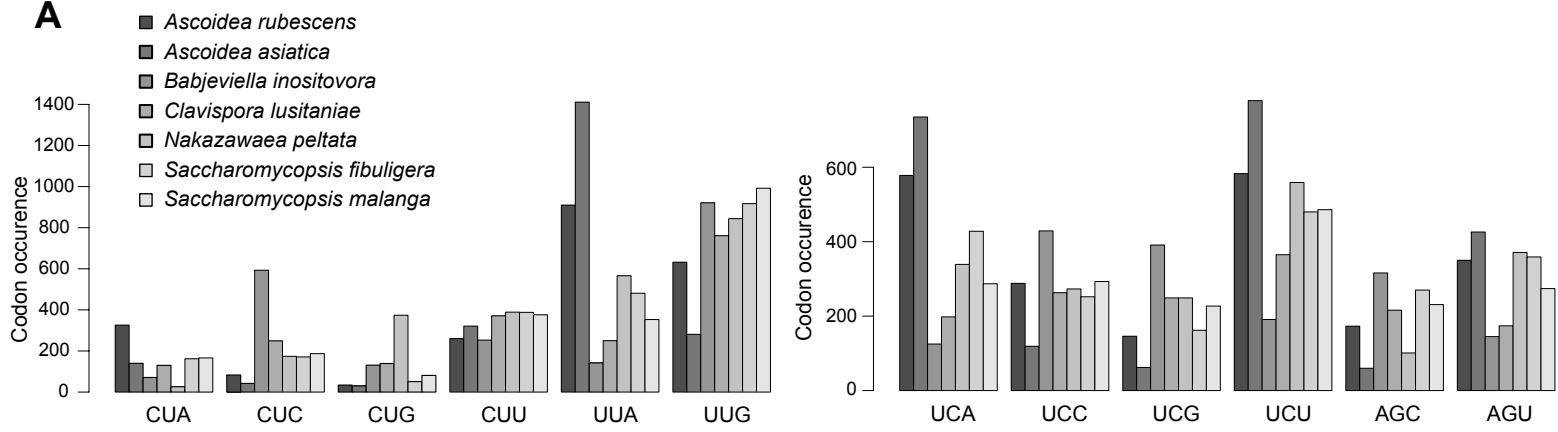
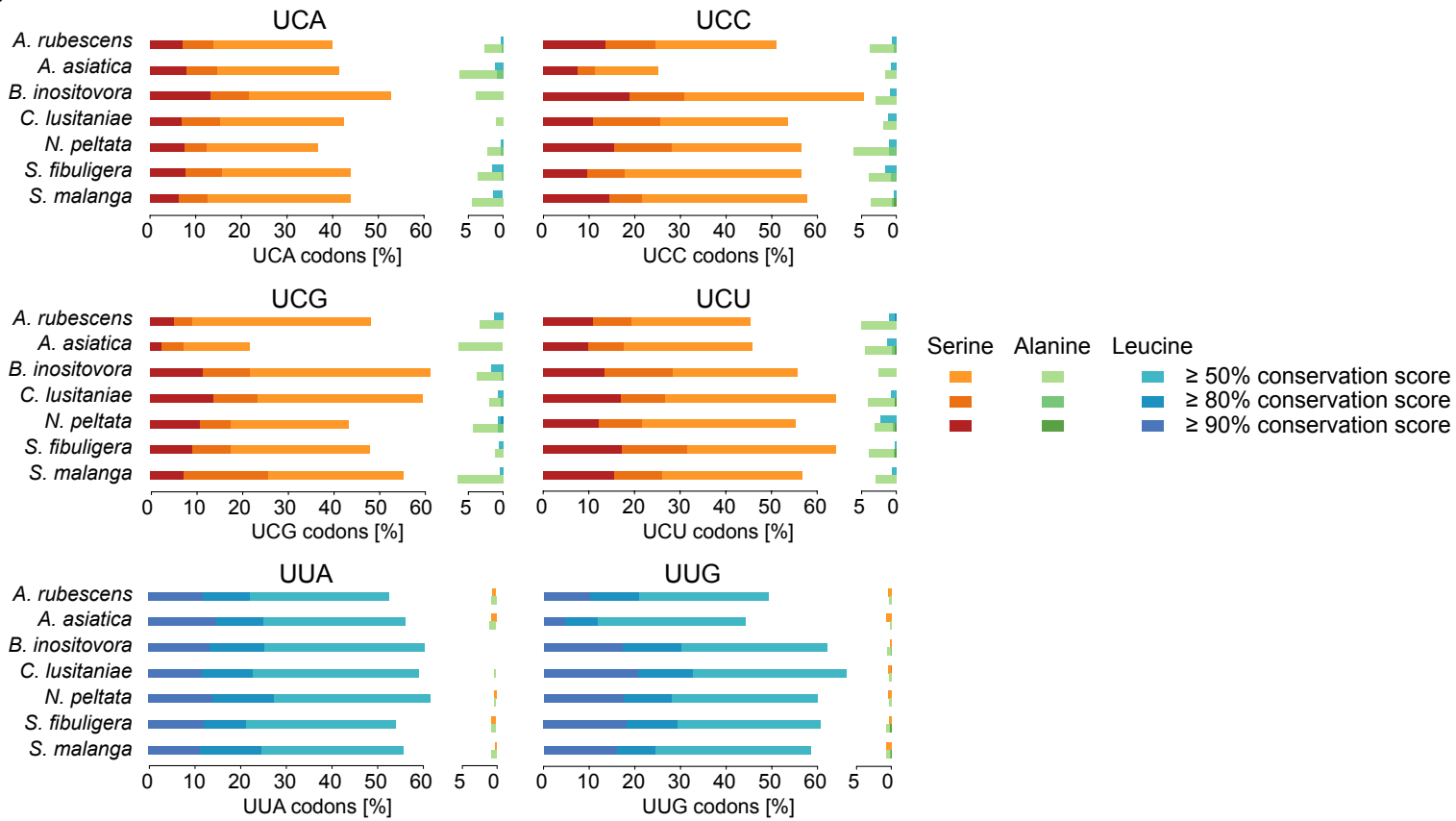
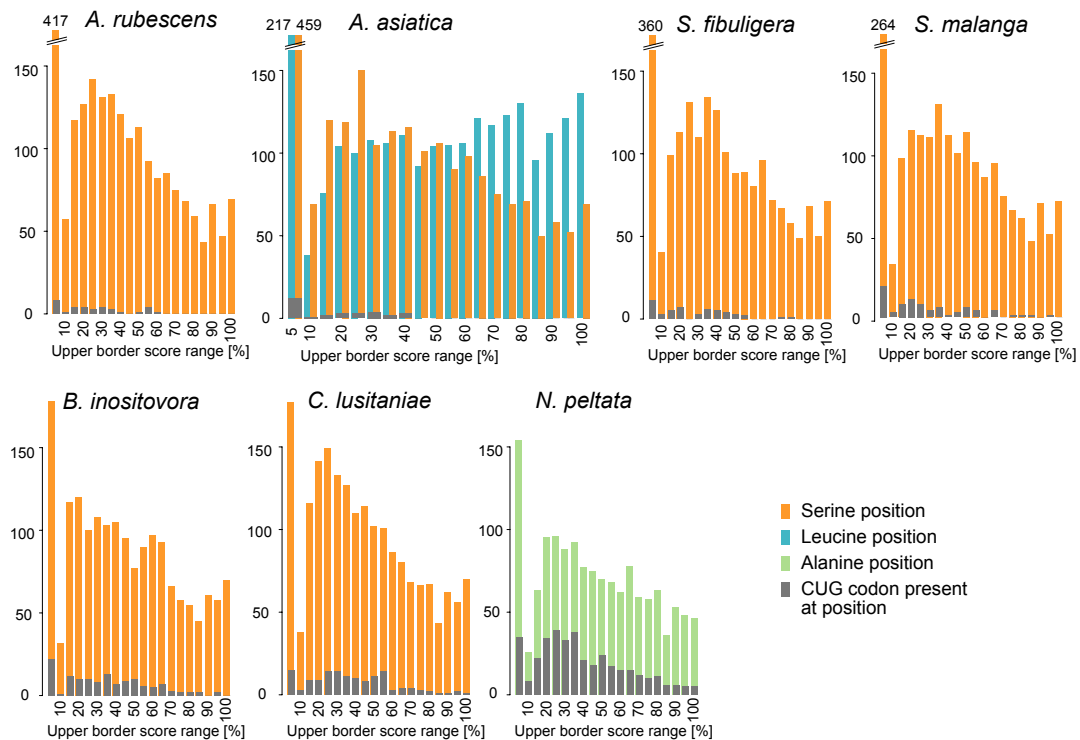
A**B****C**

Figure S3. Number and conservation of leucine and serine codons in the cytoskeletal and motor protein sequence alignment, Related to Figure 3.

A) Occurrence of each of the leucine and serine codons in the alignment. B) Percentages of selected leucine and serine codons present at alignment positions of a certain conservation score. On the left, codons found at alignment positions enriched in the expected amino acid are shown, contrasted by codons found at alignment positions enriched in an unexpected amino acid on the right. Leucine and serine codons not shown here are part of Figure 3 of the main manuscript. C) Number of serine/ leucine/ alanine alignment positions falling into a score range. The number of those positions that contain at least one CUG codon is plotted in front. For *A. asiatica*, alignment positions with both serine and leucine have been considered.

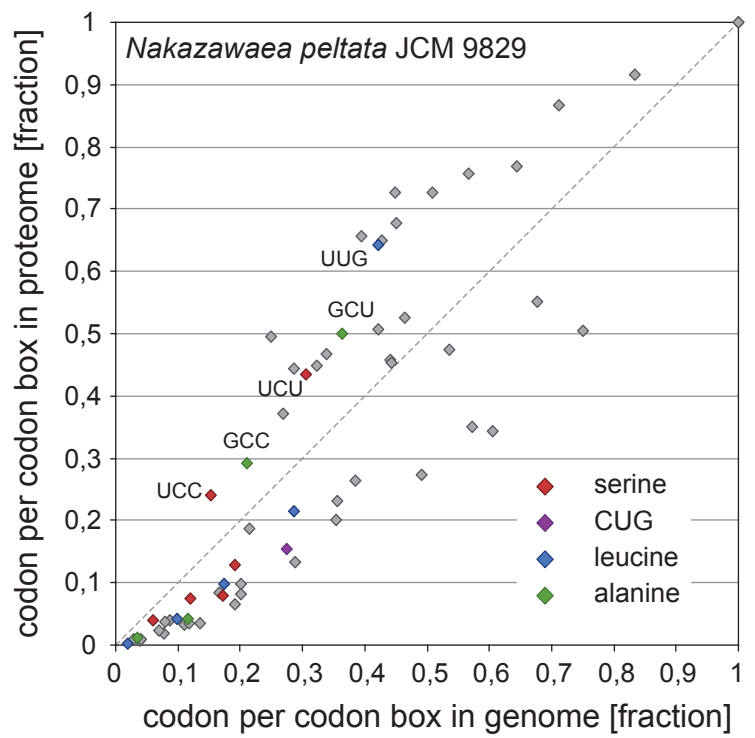
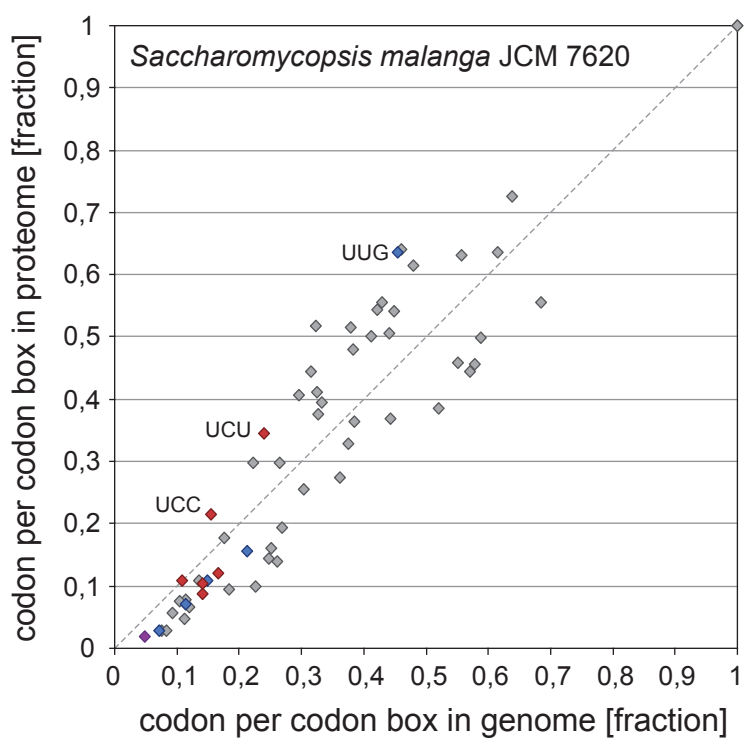
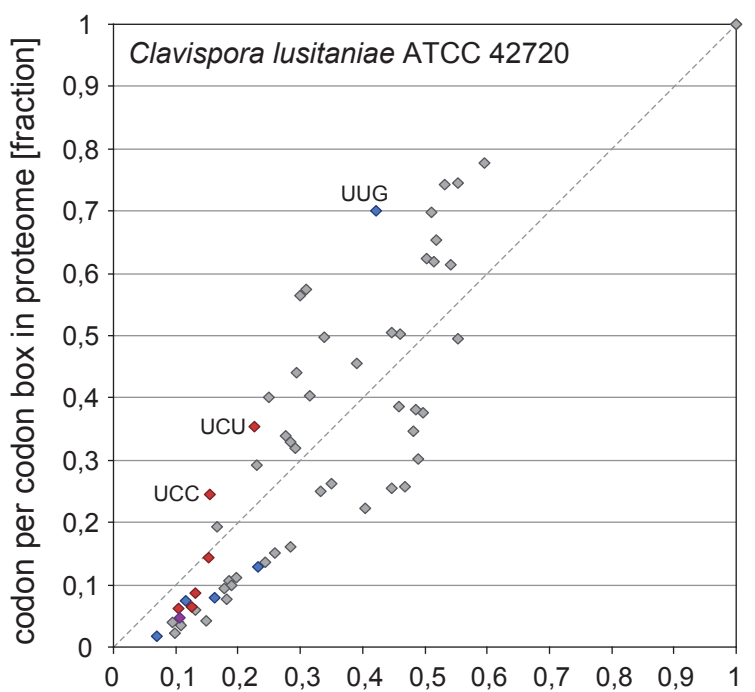
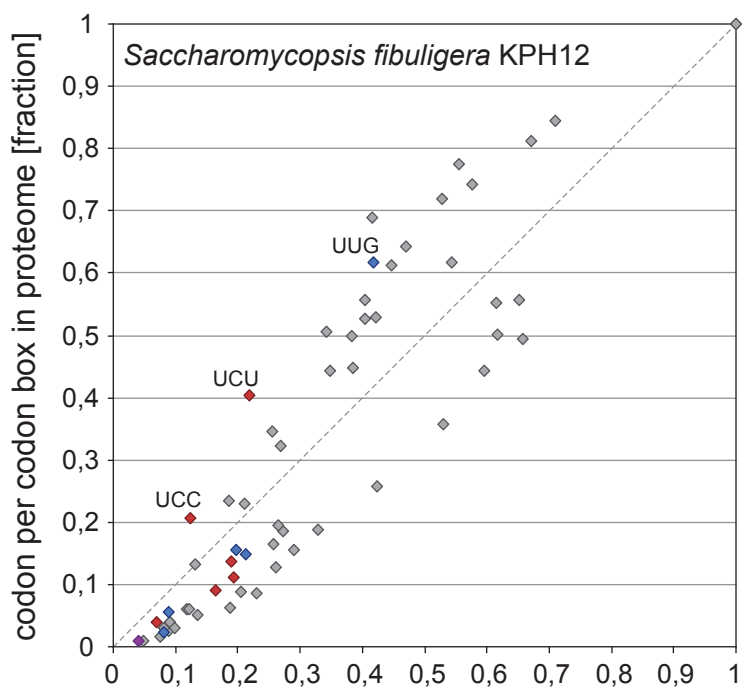
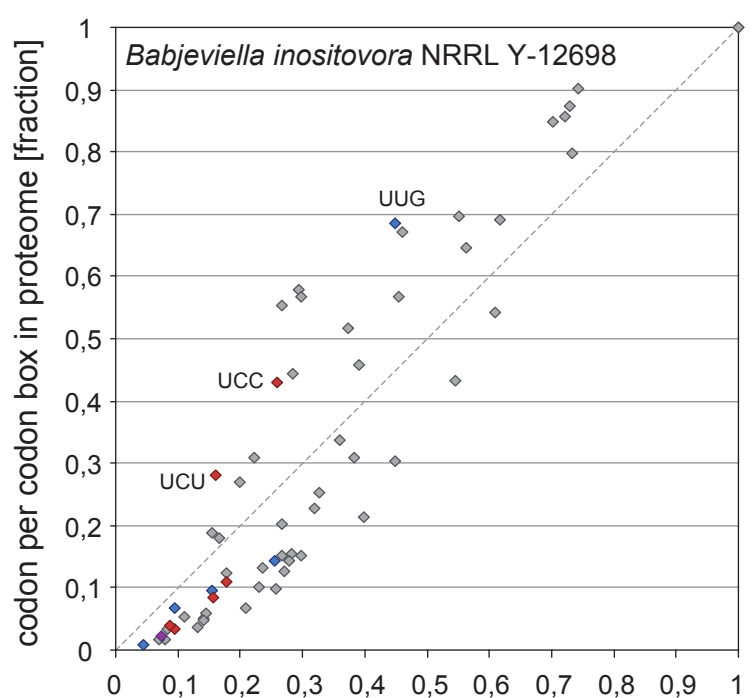
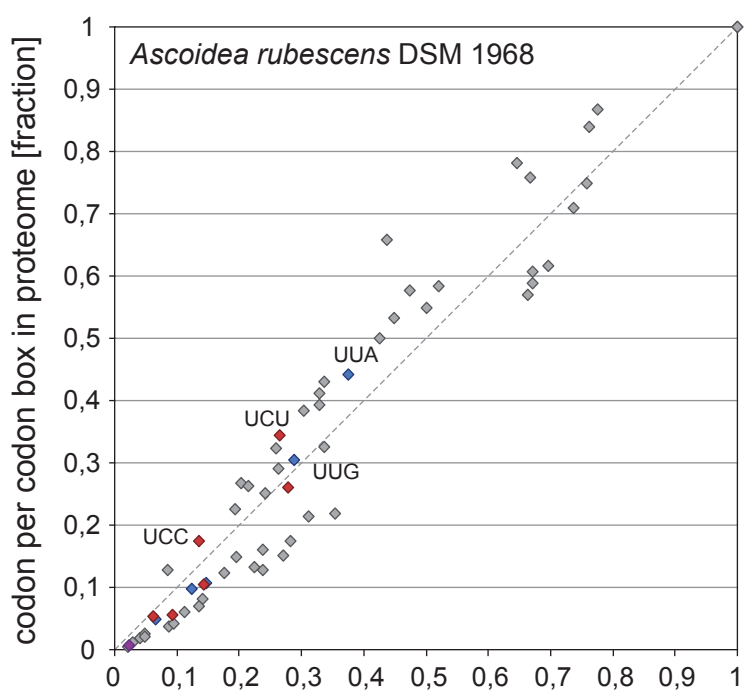


Figure S4. Codon usage in genome versus proteome, Related to Figure 4.

The scatter plots present the fraction of each codon per family box according to its usage in the genome, determined by analysis of the gene prediction datasets, versus its usage in the proteome, determined by analysis of the MSMS data. Serine, leucine, and alanine family box codons, and the CUG codons are highlighted by red, blue, green and purple colour, respectively. If the proteins found in the proteome were representative of the genome, all codons should be on the diagonal. However, the expressed proteins are encoded by preferred codons (upper left triangle), while other codons are considerably less used (lower right triangle). The CUG codons are all in the lower right triangle, meaning that they are mostly present in genes whose proteins were not detected in the proteomics analyses. Serine and leucine (and alanine in case of *N. peltata*) codons preferably used in the proteome are indicated for orientation.

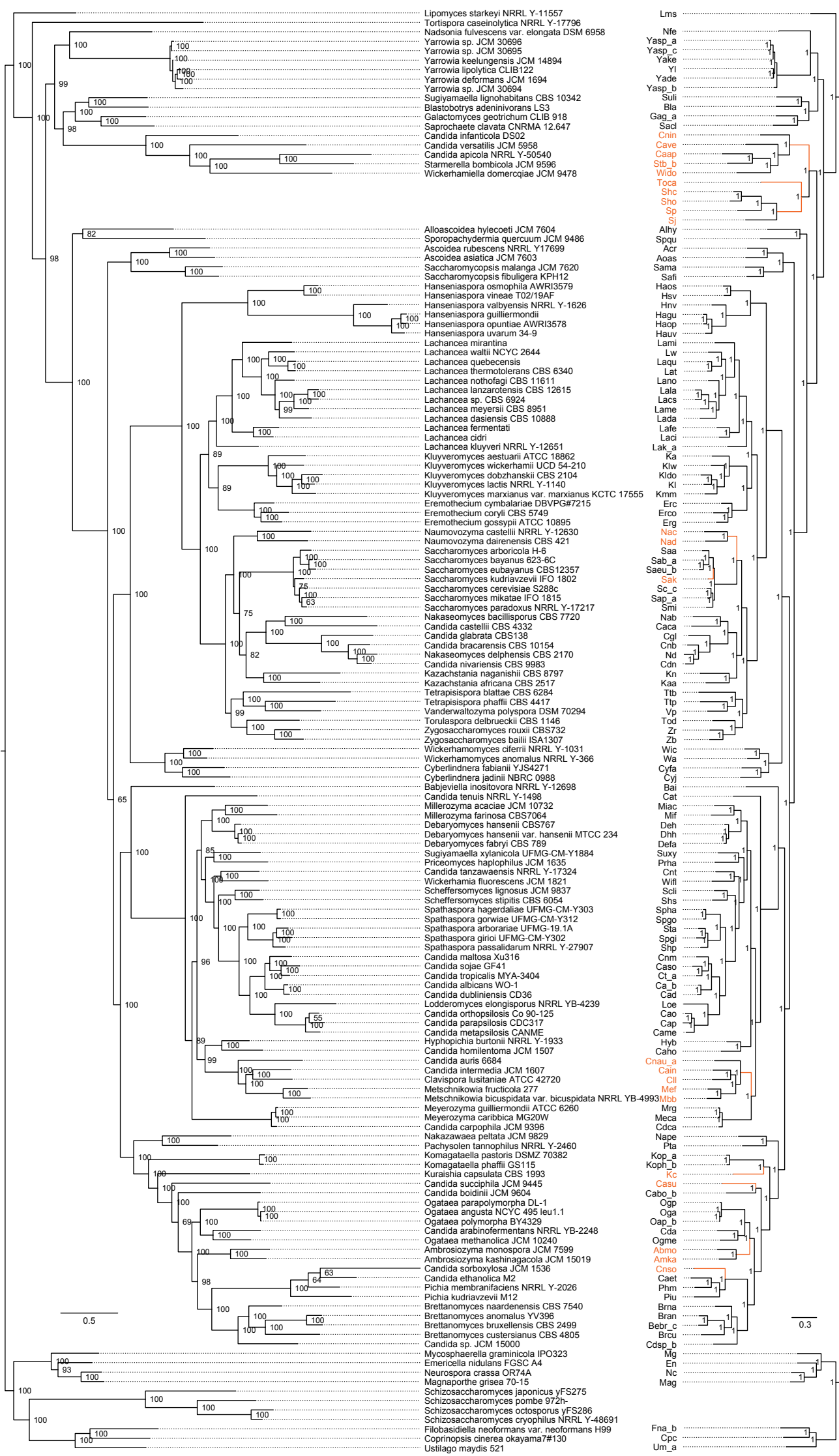


Figure S5. Contrasting species trees generated with the Maximum-Likelihood and the Bayesian approach, Related to Figure 5.

Left tree: RAxML generated tree with LG +G +I substitution model and 1000 bootstrap replicates. Right tree: MrBayes generated tree with mixed amino acid model and posterior probabilities given for branch support. Species and internal branchings differing between MrBayes and RAxML generated trees are indicated in red color in the MrBayes tree.

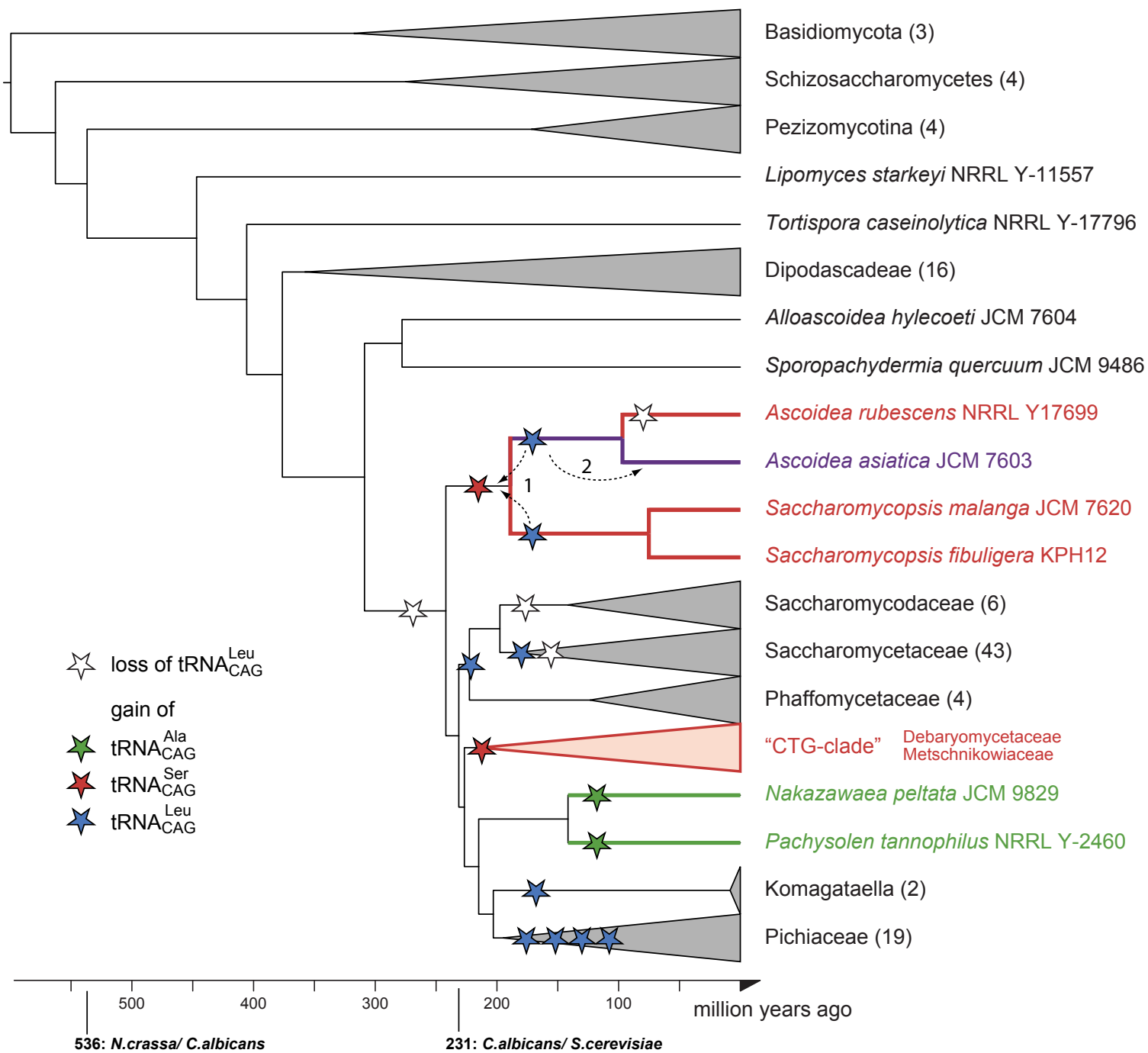


Figure S6. Dating tRNA-loss and -gain events, Related to Figure 5.

Dated RAxML generated tree with $tRNA_{CAG}^{Leu}$ loss and gain events marked. The $tRNA_{CAG}^{Leu}$ gain and loss events are placed according to [S1]. The multiple $tRNA_{CAG}^{Leu}$ gain events in the Pichiaceae branch indicate multiple independent gains within this branch, as detailed in [S1] (see also the Leu tRNA phylogeny plot on FigShare). In an alternative scenario (“1”), the *Ascoidea* clade $tRNA_{CAG}^{Leu}$ have a common origin. In a second alternative scenario (“2”), the $tRNA_{CAG}^{Leu}$ could have been independently acquired by *A. asiatica* and the ancestor of the *Saccharomycopsis* yeasts, in which case *A. rubescens* never had this tRNA. Divergence times were estimated by TreePL based on constrains set on the splits between *Neurospora crassa* and *Candida. albicans* (536 million years ago) and *C. albicans* and *S. cerevisiae* (231 million years ago).

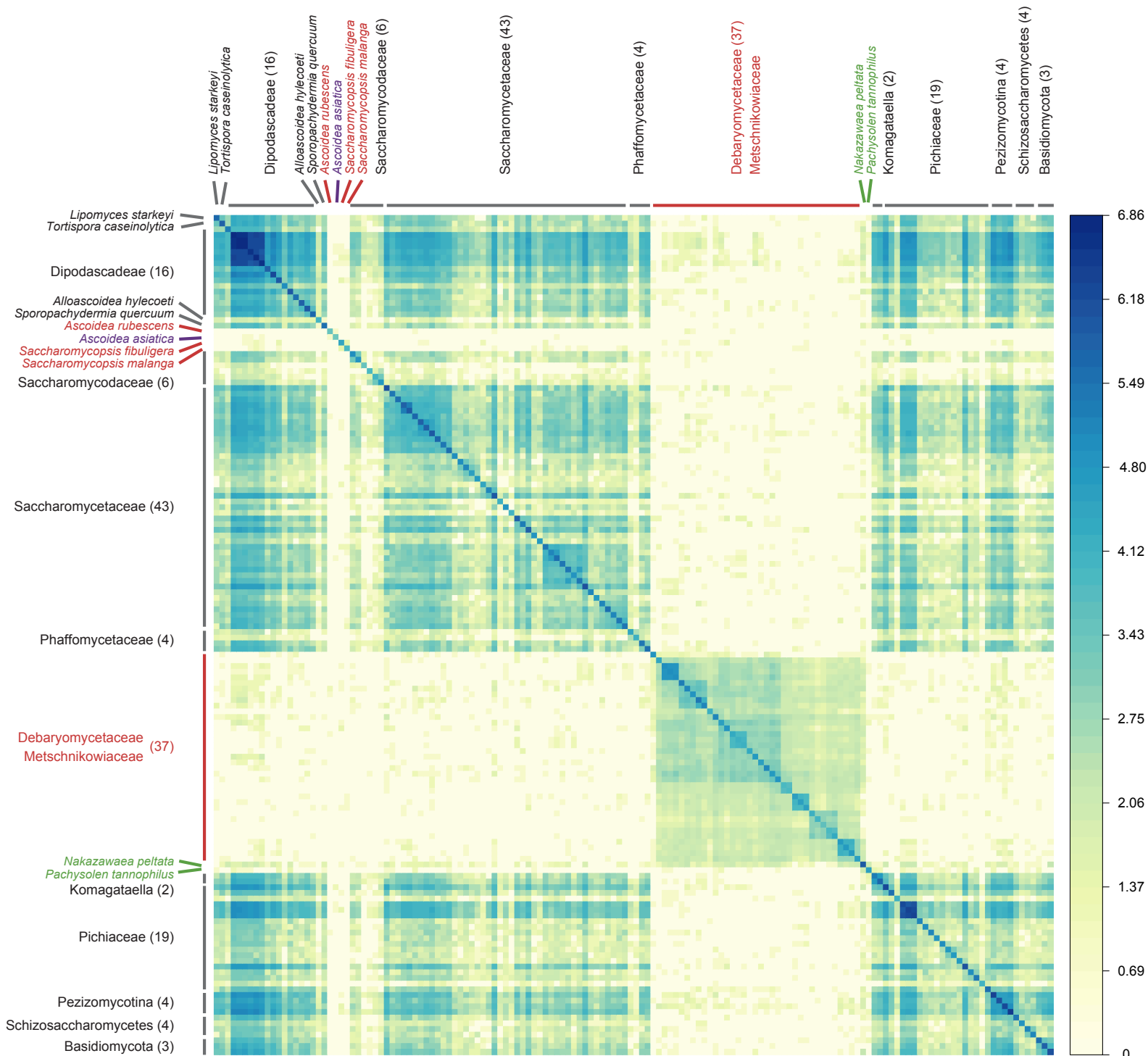


Figure S7. Common CUG positions in 26 cytoskeletal and motor proteins of 148 fungi, Related to Figure 6.

The diagonal denotes the total number of CUG positions. For displaying purposes, numbers have been log transformed. Some species names have been omitted and instead, the group name and number of species inside that group are given.

Supplemental References

- S1. Mühlhausen, S., Findeisen, P., Plessmann, U., Urlaub, H., and Kollmar, M. (2016). A novel nuclear genetic code alteration in yeasts and the evolution of codon reassignment in eukaryotes. *Genome Res.* 26, 945–955.